



## Key drivers of ozone change and its radiative forcing over the 21st century

5 **Fernando Iglesias-Suarez<sup>1,2</sup>, Douglas E. Kinnison<sup>3</sup>, Alexandru Rap<sup>4</sup>,  
Oliver Wild<sup>1,2</sup> and Paul J. Young<sup>1,2,5</sup>**

<sup>1</sup>Lancaster Environment Centre, Lancaster University, Lancaster, UK

<sup>2</sup>Data Science Institute, Lancaster University, Lancaster, UK

<sup>3</sup>Atmospheric Chemistry Observations and Modeling Laboratory, National Center for Atmospheric Research, Boulder, Colorado, USA

10 <sup>4</sup>School of Earth and Environment, University of Leeds, Leeds, UK

<sup>5</sup>Pentland Centre for Sustainability in Business, Lancaster University, Lancaster, UK

Correspondence to: F. Iglesias-Suarez ([n.iglesiassuarez@lancaster.ac.uk](mailto:n.iglesiassuarez@lancaster.ac.uk))

### Abstract

15 Over the 21st century changes in both tropospheric and stratospheric ozone are likely to have important consequences for the Earth's radiative balance. In this study we investigated the radiative effects of future ozone changes, using the Community Earth System Model (CESM1), with the Whole Atmosphere Community Climate Model (WACCM), and including fully coupled radiation and chemistry schemes. Using year  
20 2100 conditions from the Representative Concentration Pathways 8.5 (RCP8.5) scenario, we quantified the individual contributions to ozone radiative forcing of (1) climate change (with and without lightning feedback), (2) reduced concentrations of ozone depleting substances (ODSs), and (3) methane increases. We calculated future ozone radiative forcing relative to year 2000 of (1)  $63 \pm 76 \text{ mWm}^{-2}$ , (2)  
25  $129 \pm 81 \text{ mWm}^{-2}$ , and (3)  $225 \pm 85 \text{ mWm}^{-2}$ , due to climate change, ODSs and methane respectively. Our best estimate of net ozone forcing in this set of simulations is  $420 \pm 120 \text{ mWm}^{-2}$  relative to year 2000, and  $750 \pm 230 \text{ mWm}^{-2}$  relative to year 1750, with uncertainty range given by approximately  $\pm 30\%$ . We find that the overall long-term tropospheric ozone forcing from methane chemistry-climate feedbacks



related to OH and methane lifetime is small ( $46 \text{ mWm}^{-2}$ ). Ozone forcings associated with climate change and stratospheric ozone recovery are robust with regard to background conditions, even though the ozone response is sensitive to both changes in atmospheric composition and climate. Changes in stratospheric-produced ozone account for  $\sim 47\%$  of the overall radiative forcing in this set of simulations, highlighting the key role of the stratosphere in determining future radiative forcing.

## 1 Introduction

Ozone is an important trace gas that plays a key role in the Earth's radiative budget, atmospheric chemistry and air quality. As a radiatively active species, ozone interacts with both shortwave and longwave radiation. In the troposphere, ozone is an important regulator of the oxidising capacity (both itself and as the main source of hydroxyl radicals, OH), as well as being an important pollutant, with negative effects on vegetation and human health (e.g. Prather et al., 2001; UNEP, 2015). However, approximately 90% of ozone is found in the stratosphere – protecting the biosphere from harmful ultraviolet solar radiation (WMO, 2014) – and is an important source of ozone in the troposphere and its budget (e.g. Collins et al., 2003; Sudo et al., 2003; Zeng and Pyle, 2003). Therefore, its future evolution – in the troposphere and the stratosphere – is a main concern for climate change and air quality during the 21st century. Future changes in emissions of ozone precursors (e.g. methane), ozone depleting substances (ODSs) and climate are thought to be major drivers of ozone abundances (e.g. Stevenson et al., 2006; Kawase et al., 2011; Young et al., 2013; Banerjee et al., 2016).

Stratospheric-tropospheric exchange (STE) of ozone significantly influences the abundance and distribution of tropospheric ozone (e.g. Banerjee et al., 2016). Although, observational estimates and climate models suggest an acceleration of the stratospheric mean mass transport via the Brewer-Dobson circulation (BDC) associated with climate change (e.g. Oberländer et al., 2013; Ploeger et al., 2013; Butchart, 2014; Stiller et al., 2017), significant uncertainty still remains (Engel et al., 2009; Hegglin et al., 2014; Ray et al., 2014). The BDC is the wave-driven factor governing the transport of air and trace constituents in the stratosphere, and characterized by upwelling in the tropics, poleward motion in the stratosphere and



sinking at middle and high latitudes (Butchart, 2014, and references therein). The BDC is commonly thought to consist of a shallow branch, controlling the lower stratosphere region, and a deep branch controlling the middle and upper stratosphere. The latter presents two cells during the spring and fall seasons, and one stronger cell  
5 into the winter hemisphere (Birner and Bönisch, 2011). The tropopause is the boundary that “separates” the troposphere and the stratosphere, two chemically and dynamically distinct regions. Defining the tropopause is crucial to diagnose budget terms of trace gases such as the STE of ozone (e.g. Prather et al., 2011), although the chosen definition may affect the resulting analysis (e.g. Wild, 2007; Stevenson et al.,  
10 2013; Young et al., 2013).

Stratospheric ozone is expected to recover to pre-industrial levels during the 21st century due to the implementation of the Montreal Protocol and its Amendments and Adjustments (WMO, 2014), as ODSs concentrations slowly decrease in the atmosphere (e.g. Austin and Wilson, 2006; Eyring et al., 2010). Indeed, the global  
15 ozone layer has already shown the first signs of recovery (WMO, 2014; Chipperfield et al., 2017). Future ozone recovery can affect tropospheric composition via enhanced STE of ozone and reductions in tropospheric photolysis rates, both associated with higher levels of ozone in the stratosphere. Previous modelling studies that have isolated the impacts of stratospheric ozone recovery have shown that the increased  
20 STE is the most important driver of changes in the tropospheric ozone burden (Zeng et al., 2010; Kawase et al., 2011; Banerjee et al., 2016). However, reductions in ozone photolysis result in lower OH concentrations – i.e.  $\text{O}_3 + h\nu (\lambda < 320 \text{ nm}) \rightarrow \text{O}(^1\text{D}) + \text{O}_2$  – and therefore longer methane lifetime (e.g. Morgenstern et al., 2013; Zhang et al., 2014).

25 Impacts of future climate change on ozone are robust across a number of modelling studies and multi-model activities (Kawase et al., 2011; Young et al., 2013; Arblaster et al., 2014; Banerjee et al., 2016; Iglesias-Suarez et al., 2016). Stratospheric cooling leads to further ozone loss in the lower stratosphere (through enhanced heterogeneous ozone destruction) and ozone increases in the upper  
30 stratosphere (through reduced  $\text{NO}_x$  abundances and  $\text{HO}_x$ -catalysed ozone loss, and enhanced net oxygen chemistry) (Haigh and Pyle, 1982; Rosenfield et al., 2002). In addition, a projected acceleration of the BDC leads to an enhanced STE of ozone (e.g. Garcia and Randel, 2008; Butchart et al., 2010), which results in (i) decreases in



tropical lower stratospheric ozone, associated to an increase of relatively ozone-poor air entering from the troposphere; and (ii) ozone increases in the upper troposphere, particularly in the region of the subtropical jets, linked to the descending branch of the BDC. On the other hand, a warmer and wetter climate results in lower tropospheric  
5 ozone levels – i.e. linked to a decrease in net chemical production due to enhanced ozone chemical loss – (e.g. Wild, 2007).

Climate feedbacks associated with future ozone changes are surrounded by large uncertainties. Lightning is a major natural source of nitrogen dioxides ( $\text{LNO}_x$ ) in the troposphere and the only source away from the surface (Galloway et al., 2004),  
10 with important consequences for atmospheric composition in the mid-upper troposphere and the lower stratosphere. The current best estimate of annual and global mean  $\text{LNO}_x$  emissions is  $5 \pm 3 \text{ Tg(N) yr}^{-1}$ , with chemistry-climate models suggesting  $\text{LNO}_x$  emissions sensitivity to climate change of  $\sim 4\text{--}60 \text{ \% K}^{-1}$  (Schumann and Huntrieser, 2007). Although more recent modelling studies find  $\text{LNO}_x$  emissions  
15 climate sensitivity lying at the lower end of the above estimate (Zeng et al., 2008; Banerjee et al., 2014), results from a multi-model activity suggest large uncertainty in the magnitude and even the sign of future projections response due to different parameterizations (Finney et al., 2016). Most  $\text{LNO}_x$  emissions occur in the mid-upper  
20 tropical troposphere over the continents, where photochemical production of ozone is most efficient in the troposphere – i.e. low background concentrations and longer lifetimes of  $\text{NO}_x$ , lower temperatures affecting ozone loss chemistry and abundant sunlight (e.g. Williams, 2005; Dahlmann et al., 2011). A small but significant fraction of lightning-induced  $\text{NO}_x$  emissions are converted into less photochemically active nitric acid ( $\text{HNO}_3$ , via  $\text{HO}_2 + \text{NO}$  reaction), which can be removed through wet  
25 deposition or transported into the lower stratosphere (acting as a reservoir of  $\text{NO}_x$ ) (e.g. Jacob, 1999; Søvde et al., 2011). In addition, OH concentrations increase with  $\text{LNO}_x$  emissions and the resultant lightning-produced ozone – i.e. via  $\text{NO} + \text{HO}_2$  and  $\text{O}(^1\text{D}) + \text{H}_2\text{O}$  respectively – with a corresponding reduction in methane lifetime. This resulting climate feedback is important because methane is a potent GHG and ozone  
30 precursor.

To date, ozone is the third largest contributor to the total radiative forcing (RF) since the pre-industrial period, with its overall increases contributing  $+0.35 \text{ Wm}^{-2}$  (Myhre et al., 2013). We use the concept of radiative effect (RE) to



diagnose the impact of ozone abundances and distributions on the atmospheric radiative budget. The ozone RE is the radiative flux imbalance between incoming shortwave solar radiation and outgoing longwave infrared radiation (at the tropopause, after allowing for stratospheric temperatures to readjust to radiative equilibrium) which results from the presence of both anthropogenic and natural ozone (Rap et al., 2015). Note that RF is therefore the change in RE over time (e.g. Myhre et al., 2013). Ozone shows two distinct regimes with regard to its RE, with positive (longwave radiation) and negative (shortwave radiation) effects for increases in stratospheric ozone, and positive (for both longwave and shortwave radiation) effects for ozone increases in the troposphere (e.g. Lacis et al., 1990; Forster and Shine, 1997). In addition, changes in ozone distribution – i.e. latitudinal and vertical structure – are of a particular interest for its RE, due to horizontally varying factors such as, surface albedo, clouds and the thermal structure of the atmosphere (e.g. Lacis et al., 1990; Berntsen et al., 1997; Forster and Shine, 1997; Gauss et al., 2003). Previous studies showed highest radiative efficiency of ozone in the tropical upper troposphere (e.g. Worden et al., 2011; Riese et al., 2012; Rap et al., 2015), a region greatly influenced by stratospheric influx (e.g. Hegglin and Shepherd, 2009; Zeng et al., 2010) and lightning-produced ozone (e.g. Liaskos et al., 2015).

Modelling experiments used in the latest Assessment Report of the Intergovernmental Panel on Climate Change (IPCC) followed the Representative Concentration Pathways (RCPs) emission scenarios for short-lived precursors (van Vuuren et al., 2011) and long-lived species (Meinshausen et al., 2011). The RCPs are named according to the total radiative forcing at the end of the 21st century relative to 1750. For example, the RCP8.5 emission scenario refers to the total  $8.5 \text{ Wm}^{-2}$  RF by 2100. To different extents, all RCPs adopt future global stringent air quality regulations by 2100 relative to year 2000, resulting in reductions of  $\text{NO}_x$  and Non Methane Volatile Organic Compounds (NMVOCs) emissions. However, methane emissions decrease in all RCPs but for RCP8.5 – i.e. more than doubled emissions are assumed – for the same period.

Previous research has investigated impacts on ozone abundances and distributions associated to future changes in climate, ODSs and ozone precursor emissions in a processed-based approach (Collins et al., 2003; Sudo et al., 2003; Zeng and Pyle, 2003; Zeng et al., 2008; Zeng et al., 2010; Kawase et al., 2011; Banerjee et



al., 2016). Other modelling studies focused on the radiative effects of mainly tropospheric ozone changes under future emission scenarios in a non processed-based fashion (e.g. Gauss et al., 2003; Stevenson et al., 2013). One study has recently identified the indirect tropospheric and stratospheric ozone RF between 2000 and 2100 due to individual perturbations (Banerjee et al., 2017). Yet the upper limit of future ozone RF remains poorly constrained. For example, climate models do not even necessarily agree on the sign of the indirect ozone forcing resulting from climate change and associated feedbacks (i.e. LNO<sub>x</sub>). Furthermore, there are uncertainties arising from the interactions and non-linearities between different agents (i.e. combined forcing may differ from the sum of individual forcings due to different background conditions), as well as and long-term changes (i.e. methane feedback associated with changes in lifetimes).

Here we aim to narrow this gap by assessing how key factors drive net ozone radiative forcing, and provide a gauge of the uncertainty arising from non-linearities and long-term feedbacks. We use the Community Earth System Model (CESM1) in its “high-top” (up to 140 km) atmosphere version – the Whole Atmosphere Community Climate Model (WACCM) – and a series of sensitivity simulations to quantify the radiative effects of ozone due to future climate change, stratospheric ozone recovery, and methane emissions between 2000 and 2100. Particular attention is given to non-linearities emerging from climate change and ozone recovery, lightning-produced ozone (i.e. climate feedback surrounded with large uncertainties), methane emissions due to its GHG and ozone precursor dual role, and the contribution from the stratosphere on tropospheric ozone under the RCP8.5 emission scenario. Moreover, here we use a synthetic ozone tracer to unambiguously identify for the first time stratospheric- and tropospheric-produced ozone forcing. The CESM1-WACCM model, sensitivity simulations and ozone radiative effect calculations are described in Section 2. Results of future projected ozone changes and associated radiative effects are presented in Sect. 3 and 4, respectively. Different sources of uncertainties are discussed and accounted for in Sect. 5. Finally, a summary and concluding remarks are presented in Sect. 6.



## 2 Methodology

### 2.1 Model description

We use the CESM version 1.1.1 with a configuration that fully couples the  
5 atmosphere and land components. A comprehensive description of the model is given  
by Marsh et al. (2013, and references therein).

The atmosphere component is WACCM version 4, a high-top model that  
extends from the surface to approximately 140 km in the lower thermosphere, with a  
vertical resolution ranging from 1.2 km near the tropopause to ~ 2 km near the  
10 stratopause, and horizontal resolution of 1.9° x 2.5° (latitude by longitude). The  
chemical scheme is the Model for Ozone and Related Chemical Tracers (MOZART)  
for the troposphere (Emmons et al., 2010) and the stratosphere (Kinnison et al., 2007),  
including recent updates (Lamarque et al., 2012; Tilmes et al., 2015). It includes 169  
chemical species with detailed photolysis, gas-phase and heterogeneous reactions (see  
15 Tables A1 and A2 in Tilmes et al., 2016). Recent updates in the orographic gravity  
wave forcing – reducing the cold bias in Antarctic polar temperatures – (Calvo et al.,  
2017; Garcia et al., 2017) and the polar stratospheric chemistry (Wegner et al., 2013;  
Solomon et al., 2015) are included in the model. Concentrations of radiatively active  
gas-phase compounds such as ozone, nitrous oxide (N<sub>2</sub>O), methane (CH<sub>4</sub>) and other  
20 ODSs, are coupled to the model radiation scheme. Lightning-induced NO<sub>x</sub> (LNO<sub>x</sub>)  
emissions are parameterized using the cloud top height method (Price and Vaughan,  
1993), and annual global mean LNO<sub>x</sub> emissions are scaled to simulate present-day  
values of between 3-5 Tg N yr<sup>-1</sup>.

A stratospheric ozone tracer (O3S) is implemented to represent the abundance  
25 and distribution of stratospheric-produced ozone in the troposphere (Roelofs and  
Lelieveld, 1997). O3S is equivalent to ozone in the stratosphere. In the troposphere it  
undergoes the same chemical loss processes as ozone, but does not undergo dry  
deposition, following the recommendations for the Chemistry-Climate Model  
Initiative (CCMI) (Eyring et al., 2013; Morgenstern et al., 2017). We apply an annual  
30 global correction factor to account for the dry deposition of O3S based on an  
additional model simulation. This correction factor is approximately linear, ranging  
from 0.7 at the surface to 0.95 around 250 hPa.



The land component is the Community Land Model version 4 which has the same horizontal resolution as the atmosphere component, and interactively calculates dry deposition for trace gases in the atmosphere (Val Martin et al., 2014) and biogenic emissions using the Model of Emissions of Gases and Aerosols from Nature (MEGAN) version 2.1 (Guenther et al., 2012).

## 2.2 Experimental setup

This study uses time slice simulations driven by sea surface temperatures (SSTs) and sea ice climatologies from previous CESM1-WACCM fully coupled simulations (SENC2-8.5; see Morgenstern et al., 2017): 1990-2009 to represent the year 2000, and 2080-2099 to represent the end of the 21st century (nominally 2100). Each time slice experiment is integrated for 20 years, using the last 10 years in this study (i.e. the spin-up period covered the first 10 years). Seasonally varying boundary conditions are specified for carbon dioxide ( $\text{CO}_2$ ),  $\text{N}_2\text{O}$ ,  $\text{CH}_4$ , and ODSs (halogen-containing compounds), and the MACCity data set (Granier et al., 2011) is used to specify anthropogenic  $\text{NO}_x$ ,  $\text{CO}$ , and NMVOC emissions, as recommended for CCM1 (Eyring et al., 2013). Volcanic eruptions are not included in the experiments, and the incoming solar radiation is fixed at  $1361 \text{ Wm}^{-2}$ . The quasi-biennial oscillation is imposed by relaxation of equatorial winds (90-3 hPa) with an approximate 28-month period between eastward and westward phase (Marsh et al., 2013).

Table 1 lists the simulations used in this study. The control simulation (CNTRL) had all boundary conditions set to the year 2000, and a set of sensitivity simulations had one (or more) boundary condition(s) changed to the year 2100. The simulations can be classified into three main groups:

1. Sensitivity simulations that explore the impacts of climate change. Here SSTs, sea ice and main GHGs (i.e.  $\text{CO}_2$  and  $\text{N}_2\text{O}$ ) are specified to year 2100 levels. The upper end emission scenario of the RCPs family is explored (RCP8.5). Natural biogenic emissions (e.g. isoprene) are calculated online, which are mainly governed by changes in  $\text{CO}_2$ , climate and land use (Squire et al., 2014). The indirect ozone radiative effect resulting from this climate feedback is implicitly contained in the climate signal. However, unlike  $\text{LNO}_x$  emissions it mainly impacts ozone in the lower troposphere, where ozone shows relatively small radiative efficiency (Rap et al., 2015). To isolate the impacts





- of lightning-produced ozone, additional experiments are performed with year 2000 levels for LNO<sub>x</sub> emissions (fLNO<sub>x</sub>). Fixed LNO<sub>x</sub> simulations follow the Banerjee et al. (2014) approach, imposing the monthly mean LNO<sub>x</sub> emissions climatology from the CNTRL run and switching off its interactive calculation
- 5 in the model. To justify this method, we compared temperature and tropospheric ozone fields between the CNTRL and CNTRL-fLNO<sub>x</sub> simulations and found negligible differences (not shown).
2. Stratospheric ozone recovery due to the slow decrease of ODSs (referring to the total organic chlorine and bromine species) concentrations regulated under the framework of the Montreal Protocol is investigated. Based on the CCMI

10 recommendations, halogen species (CFC11, CFC12, CFC113, CFC114, CFC115, CCl<sub>4</sub>, HCFC22, HCFC141b, HCFC142b, CF<sub>2</sub>ClBr, CF<sub>3</sub>Br, CH<sub>3</sub>Br, CH<sub>3</sub>CCl<sub>3</sub>, CH<sub>3</sub>Cl, H1202, H2402, CH<sub>2</sub>Br<sub>2</sub>, and CHBr<sub>3</sub>) are specified to year 2100 levels for the halogen scenario A1 (WMO, 2011), which includes the

15 early phase-out of hydrochlorofluorocarbons agreed in 2007. Note that two brominated short-lived species (CH<sub>2</sub>Br<sub>2</sub> and CHBr<sub>3</sub>) were included in these experiments to accurately represent bromine loading and thus the associated ozone depletion, providing an additional bromine surface mixing ratio of ~ 6 pptv on top of that from the longer-lived bromine compounds.

20 3. Future levels of methane and its impacts on ozone are investigated. Concentrations of CH<sub>4</sub> are imposed to year 2100 levels from the RCP8.5 pathway – i.e. approximately double concentrations compared to year 2000. Note that methane levels were kept at year 2000 levels for the sensitivity simulations described above that explore climate change impacts.

### 25 **2.3 Radiative effect**

To calculate the RE of ozone we use the ozone radiative kernel of Rap et al. (2015). The radiative kernel is defined as the derivative of the radiative flux relative to perturbations in ozone. It is calculated by computing stratospherically adjusted ozone REs at the tropopause as a consequence of small perturbations (1 ppbv) imposed to

30 each model layer (everything else is unchanged), with respect to the reference climatology. Multiplying simulated ozone fields with the ozone radiative kernel was



shown to be an efficient and accurate method to estimate ozone REs (Rap et al., 2015).

### 3 Present-day ozone radiative effects and model validation

- 5 A detailed present-day ozone evaluation of a similar model and experimental set-up was presented by Tilmes et al. (2016). In summary, simulated monthly mean ozone shows good agreement with observational estimates within 25 % range. Zonal and annual mean tropospheric ozone shows the best agreement with observations at low and mid-latitudes ( $\pm 5$  DU), a key region for its radiative effect (e.g. Rap et al., 2015).
- 10 Likewise, zonal and annual mean stratospheric ozone agrees fairly well with satellite estimates in the Southern Hemisphere (SH) and low latitudes ( $\pm 30$  DU), but larger deviations are found at mid- and high latitudes in the Northern Hemisphere (NH), a discrepancy also apparent in the models of the Atmospheric Chemistry and Climate Model Intercomparison Project (ACCMIP) (Iglesias-Suarez et al., 2016). The
- 15 tropospheric ozone budget (production, loss, dry deposition, stratospheric input), burden and lifetime for the CNTRL simulation (see Table 2 and Fig. S1) are within previous multi-model activities estimates (Stevenson et al., 2013; Young et al., 2013; Young et al., 2017).

20 Figures 1a-1b show annual mean ozone RE calculated for the CNTRL simulation (year 2000 or “present-day” hereafter) and the Tropospheric Emission Spectrometer (TES) from July 2005 until June 2008 (05–08). TES is the first product providing ozone profiles suitable for RE studies and has been previously evaluated against other observational estimates (e.g. Osterman et al., 2008), showing small bias in the troposphere and the stratosphere of approximately 3–4 DU. The annual and

25 global ozone RE in the CNTRL simulation is  $1.38 \pm 0.1 \text{ Wm}^{-2}$  (1 standard deviation associated with interannual variability unless otherwise specified), within the TES range of 1.35–1.41  $\text{Wm}^{-2}$ . The spatial distribution of simulated and observed ozone REs are well correlated ( $r = 0.7$ ,  $p < 0.01$ ), although note that the noisier TES signal is largely the result of averaging only three years. Both the simulated and observed

30 present-day ozone REs reveal a positive poleward gradient, with a minimum in tropical regions (approximately  $20^\circ$  N/S) that is associated with the relatively low ozone levels found in the upper troposphere and lower stratosphere (see Fig. S1). A



peak is found at high latitudes in the NH, driven by transport of relatively rich tropospheric ozone air from mid-latitudes coupled with only moderate ozone depletion in the NH stratosphere. This is in contrast with a lower RE values within the SH polar vortex, driven by the larger stratospheric ozone depletion over Antarctica (Solomon et al., 2015). Figure 1c compares the CNTRL annual mean ozone RE against the TES data set. Compared to TES, the simulated annual mean tends to overestimate the RE in the NH and underestimate it in the SH, consistent with the bias in the ozone distribution (Tilmes et al., 2016). Significant biases are mainly constrained to the tropical and subtropical regions – i.e. bias is defined here when the simulated RE  $\pm 1.96$  standard error ( $\sim 95$  % confidence interval) is outside the observed range. Tropical and subtropical regions are of particular interest for future changes in ozone and its resulting radiative forcing. Nevertheless, present-day ozone REs in these regions ( $30^\circ$  N/S) are relatively small, with a large NH/SH compensation, as shown by the annual and global mean forcings.

15

## 4 Results

### 4.1 Ozone changes

Figure 2 shows annual and zonal mean ozone changes by 2100 compared to present-day (CNTRL) imposing one single perturbation at a time. The discussion below guides through these changes, presenting the results from adding each successive perturbation, and includes chemistry-climate feedbacks.

The CLIMATE simulation (Fig. 2a) shows the expected pattern of ozone response (e.g. Kawase et al., 2011; Banerjee et al., 2014). In the troposphere, ozone decreases primarily as a consequence of a warmer and more moist climate, which drives increased ozone loss via an enhanced  $O(^1D) + H_2O$  flux (Johnson et al., 2001). Reduced net chemistry production is partially offset by an increase in the STE (Table 2), driven by an enhanced BDC (Zeng and Pyle, 2003). The fingerprint of this enhanced BDC can be seen in the lower stratosphere, both for decreases in the tropics and increases at mid-latitudes, respectively associated with the enhanced ascending and descending regions (Hegglin and Shepherd, 2009). In this simulation, the 70 hPa

25  
30



tropical (20° N/S) and zonal mean upwelling (Andrews et al., 1987) increases by 3.4 % dec<sup>-1</sup> compared to CNTRL (100 year trend). This trend is in agreement with current climate models projections of  $\sim 3.2 \pm 0.7$  % dec<sup>-1</sup> between 2005–2099 following the RCP8.5 (Hardiman et al., 2014). Additional ozone depletion over the Antarctic in CLIMATE compared to CNTRL is consistent with stratospheric cooling due to enhanced GHG levels (Fig. S3a), driving enhanced heterogeneous ozone loss chemistry (WMO, 2014). In contrast, cooling in the upper stratosphere results in ozone increases associated with a slowdown of catalytic O<sub>x</sub> cycles (Haigh and Pyle, 1982; Rosenfield et al., 2002).

Future LNO<sub>x</sub> emissions (+LIGHTNING; Fig. 2b) increase by  $\sim 33$  %, which results in ozone increases mainly in the tropical and subtropical upper troposphere. However, present-day LNO<sub>x</sub> emissions have significant uncertainties and climate models do not agree even on the sign of the change due to different lightning parameterizations (Finney et al., 2016). Nevertheless, simulated present-day LNO<sub>x</sub> emissions of  $4.8 \pm 1.6$  Tg(N) yr<sup>-1</sup> lies within observationally-derived estimates, and the model's LNO<sub>x</sub> sensitivity to climate of 10.8 % K<sup>-1</sup> is at the upper end of the two standard deviation climate model range ( $8.8 \pm 2$  % K<sup>-1</sup>) (Finney et al., 2016). The net global tropospheric ozone responses to climate will be largely determined by the interplay between climate-induced ozone losses and lightning-induced ozone production.

Reductions in inorganic chlorine and bromine abundances (O3-RECOVERY; Fig. 2c) result in stratospheric ozone increases. Upper stratospheric ozone recovers largely due to decreases in ClO<sub>x</sub>-catalysed ozone destruction. Due to reduced heterogeneous ozone loss chemistry, the largest changes are found in polar regions in the lower stratosphere, with increases of  $\sim 450$  % over the Antarctic (November) and  $\sim 45$  % over the Arctic (April). Greater abundances of stratospheric ozone result in an approximately 20 % increase in the STE (Table 2) driving higher levels of tropospheric ozone, particularly at mid- and high latitudes in the SH (related to ozone hole recovery) and tropical and subtropical upper troposphere (the descending region of the BDC), which is consistent with previous model estimates (Banerjee et al., 2016). The BDC-driven increases are somewhat offset by the larger overhead ozone column reducing actinic fluxes and therefore ozone photochemical production (Table 2) (Banerjee et al., 2016).



Methane is a greenhouse gas, an ozone precursor in the troposphere and plays various roles in the stratosphere, and these processes are difficult to isolate from the rest. The +++METHANE simulation (Fig. 2d) shows a widespread increase of ozone in the troposphere, with annual and global tropospheric column ozone increase of  $15 \pm 8$  % (Table S1). Previous modelling studies reported similar increases of 10–13 % (Brasseur et al., 2006; Kawase et al., 2011). Compensation between ozone decreases in the upper stratosphere (enhanced HO<sub>x</sub>-catalysed chemistry) and increases in the lower stratosphere (smog-like chemistry and the partitioning of active/inactive chlorine) (Randeniya et al., 2002; Stenke and Grewe, 2005; Portmann and Solomon, 2007; Fleming et al., 2011; Revell et al., 2012), results in small changes of  $2 \pm 5$  % for the annual and global stratospheric column ozone.

## 4.2 Ozone radiative forcing

Figure 3 shows maps of annual mean radiative forcing between 2000 and 2100 due to changes in ozone for the whole atmosphere, along with zonal mean forcings associated with changes in the troposphere and the stratosphere for single perturbation simulations. Note that zonal mean forcings are latitudinally-weighted, allowing direct comparison with the total forcing. Annual and global mean forcing values and their standard deviation (i.e. due to ozone changes only) are listed in Table 3. Ozone radiative forcing shows strong dependence on the vertical distribution of the change (e.g. Lacis et al., 1990; Forster and Shine, 1997; Rap et al., 2015) and to a lesser extent on the horizontal distribution (e.g. Berntsen et al., 1997). Differences can be seen in both the geographical pattern of the forcing and in the magnitude related to the drivers.

The global forcing associated with CLIMATE (Fig. 3a) of  $41.3 \pm 75$  mWm<sup>-2</sup> is small and not significant. The geographical pattern shows a relatively strong and significant forcing at high latitudes in the NH, related to ozone increases in the lower stratosphere (transport from enhanced BDC) and upper stratosphere (reduced chemical loss due to cooling). However, this is outweighed by a negative tropospheric forcing in the tropics and a negative stratospheric forcing in the SH extra-tropical region. The latter is largely due to additional ozone depletion in the lower stratosphere (i.e. reduction of STE; not shown).



Future lightning-induced  $\text{NO}_x$  emissions (+LIGHTNING; Fig. 3b) shows relatively large and significant global ozone forcing of  $104.2 \pm 79 \text{ mWm}^{-2}$ , mainly the result of simulated tropospheric ozone changes of  $2.1 \pm 2.3 \text{ DU}$ . Two distinct peak regions are evident around the subtropical belts, where large ozone changes are coincident with relatively cloud-free areas, higher temperature, and a low solar zenith angle. The strongest positive forcing is found over the Sahara and Middle East deserts, associated with greater surface albedo.

Ozone recovery (++O3-RECOVERY) drives a significant forcing of  $129.2 \pm 81 \text{ mWm}^{-2}$  (Table 3). This forcing is largely confined to the mid- and high latitudes, particularly in the SH (due to ozone hole recovery), and is mainly linked to the stratosphere (Fig. 3c). Extra-tropical STE is especially important in the SH. This is demonstrated by tropospheric forcing of about  $\sim 100 \text{ mWm}^{-2}$  in this region, which is largely the result of stratospheric-produced ozone transported to the troposphere.

The +++METHANE simulation shows a large positive forcing around the subtropical belts (Fig. 3d), which is principally confined to the troposphere, as there is a compensation between changes in the lower and upper stratosphere (Fig. 2d). In the tropical and subtropical troposphere, methane is more readily oxidised due to larger OH levels, which results in relatively large ozone increases (Fig. 3d). In addition, significant forcings at high latitudes, particularly over the Arctic, are linked to the stratosphere (i.e. reduced ozone loss via decreased active/inactive chlorine partitioning).

Figure 4 shows maps of annual mean normalised tropospheric ozone radiative forcing (NRF) between 2000 and 2100 for the four sensitivity simulations. The NRF – defined here as the tropospheric ozone radiative forcing divided by the tropospheric column ozone – is a useful diagnostic to gain insight into radiative effects of ozone changes. Very similar global NRFs of  $\sim 39 \text{ mWm}^{-2}\text{DU}^{-1}$  due to climate and methane, indicates relatively evenly distributed ozone changes in the troposphere. In contrast, more localised lightning-produced ozone results in higher global NRF of  $46 \text{ mWm}^{-2} \text{DU}^{-1}$ , whereas ozone increases at high latitudes due to ozone recovery results in smaller NRF of  $35 \text{ mWm}^{-2} \text{DU}^{-1}$ . This highlights the dependence of the resulting forcings on the vertical and horizontal distribution changes of ozone.



Previous studies have shown that the radiative forcing from tropospheric and stratospheric ozone do not have distinct drivers (Søvde et al., 2011; Shindell et al., 2013). Our results support this and show that climate change, ODSs and methane have consequences for both tropospheric and stratospheric ozone radiative forcing (Table 3). In this set of simulations, changes in ozone occurring in the troposphere and the stratosphere respectively contribute ~75 % and 25 % to the total annual and global forcing of  $417.6 \pm 81 \text{ mWm}^{-2}$ .

Further insight can be gained by attributing ozone forcing based on its origin in the stratosphere or the troposphere. In these simulations, we used a stratospheric ozone tracer (see Sect. 2) to unambiguously differentiate ozone with tropospheric origin (O3T) from that with stratospheric origin (O3S). Table 3 shows such “source classified” ozone radiative forcings, using the “O3S/ozone” and “O3T/ozone” ratios for tropospheric and stratospheric forcings respectively. Stratospheric-produced ozone contributes to ~47 % of the annual and global future ozone forcing in this set of simulations, which strongly reinforces the importance of stratospheric-tropospheric interactions.

### 4.3 Methane feedback and resulting ozone forcing

Future climate change and emissions of ODSs and methane will affect the oxidising capacity of the atmosphere (e.g., via hydroxyl radicals, OH), which in turn influences the methane lifetime ( $\tau_{\text{CH}_4}$ ) on decadal time scales resulting in a “long-term” response of tropospheric ozone (e.g. Fuglestad et al., 1999; Wild and Prather, 2000; Holmes et al., 2013). The simulations considered here neglect this feedback by imposing fixed and uniform lower boundary conditions for methane of 1748 and 3744 ppbv for years 2000 and 2100 respectively. However, we can estimate how methane concentrations would have adjusted if they were free to evolve, as well as the associated ozone response and radiative forcing. Using the method described by Fiore et al. (2009, and references therein), we calculate equilibrium methane abundances,  $[\text{CH}_4]_{\text{eq}}$ , by

$$[\text{CH}_4]_{\text{eq}} = [\text{CH}_4]_{\text{CNTRL}} \times \left( \frac{\tau_{\text{CH}_4(p)}}{\tau_{\text{CH}_4(r)}} \right)^f \quad (1)$$



where CNTRL represents the fixed boundary conditions for year 2000; ( $p$ ) and ( $r$ ) refer to the perturbation and reference simulations respectively; and  $f$  is a feedback factor which accounts for the response of methane to its own lifetime. The feedback factor is explicitly calculated for WACCM using the ++O3-RECOVERY “(a)” and  
5 +++METHANE “(b)” simulations, as follows

$$f = \frac{1}{(1 - s)} \quad (2)$$

where  $s$  is calculated by

$$s = \frac{[\ln(\tau_{\text{CH}_4(\text{b})}) - \ln(\tau_{\text{CH}_4(\text{a})})]}{[\ln(\text{BCH}_4(\text{b})) - \ln(\text{BCH}_4(\text{a}))]} \quad (3)$$

and where BCH<sub>4</sub> is the annual and global mean methane burden. We calculate a value of  $f$  of 1.43 which is at the mid-upper end of the literature range (1.19–1.53) (Prather et al., 2001; Stevenson et al., 2013; Voulgarakis et al., 2013) and within 7 % of the  
10 observationally constrained best estimate of 1.34 (Holmes et al., 2013).

The ozone response to this methane feedback is estimated by linear interpolation:

$$\Delta\text{O}_3(\text{eq} - \text{CNTRL}) = \left[ \frac{\Delta\text{CH}_4(\text{eq} - \text{CNTRL})}{\Delta\text{CH}_4(\text{b} - \text{a})} \right] \times \Delta\text{O}_3(\text{b} - \text{a}) \quad (4)$$

where  $\Delta\text{O}_3$  is the change in annual and global mean of tropospheric column ozone (Table S1). The associated tropospheric ozone forcings to methane feedback are given  
15 by the product of  $\Delta\text{O}_3$  and the NRF due to methane perturbation ( $39 \text{ mWm}^{-2} \text{ DU}^{-1}$ ; Fig. 4d) and are shown in Table 3. The overall long-term tropospheric ozone forcing related to the methane feedback in this set of simulations is a moderate increase of ~15 %. Climate change (CLIMATE and +LIGHTNING simulations) enhances the oxidising capacity of the atmosphere, which results in a small negative  
20 forcing of  $-19 \text{ mWm}^{-2}$ . In the +++METHANE simulation, OH concentrations are strongly reduced and the associated forcing of  $63 \text{ mWm}^{-2}$  outweighs the climate forcing. This forcing is within the range of ~76 (40-146)  $\text{mWm}^{-2}$  of the ACCMIP ensemble (Stevenson et al., 2013), when considering the same change in methane concentrations.

25





#### 4.4 Background conditions and forcing

Since the ozone response to a given perturbation is dependent on the background conditions (e.g. temperature, radiative heating, trace gas levels), the resulting forcing associated to individual drivers may be sensitive to the experimental design. For example, lightning-induced ozone forcing due to climate change may differ significantly under present-day or doubled methane concentrations (i.e. year 2000 or year 2100-RCP8.5 abundances). In the present study, we imposed single perturbations successively. Therefore, the total ozone forcing calculated from this set of simulations includes chemistry-climate feedbacks arising from the interactions between the various perturbations. Yet the attribution of indirect ozone forcings to individual drivers may be sensitive to the order considered (Table 1).

We also completed an additional set of simulations (Table S2) to assess the robustness of the calculated RF to the order the perturbations were applied (Table 3). Lightning-induced net ozone forcing (+LIGHTNING;  $104.2 \pm 79 \text{ mWm}^{-2}$ ) is not significantly different at the 95 % confidence interval (due to interannual variability only unless otherwise specified) compared to that calculated under approximately doubled methane concentrations (CLIMATE[CH4-2100] minus CLIMATE[CH4-2100]-fLNOx). Although the +LIGHTNING net ozone forcing is  $50 \text{ mWm}^{-2}$  lower relative to the latter, both lie within the interannual uncertainty ( $\sim 80 \text{ mWm}^{-2}$ ). The above forcing associated with ozone recovery (++O3-RECOVERY;  $129.2 \pm 81 \text{ mWm}^{-2}$ ) is calculated under climate change (i.e. including lightning feedbacks) and present-day methane concentrations, though it also can be derived under present-day climate (ODS minus CNTRL) or doubled methane concentrations (+++METHANE minus CLIMATE[CH4-2100]). We find no significant differences between the forcings associated with these background conditions, although the mean forcing resulting from the ++O3-RECOVERY is greater by  $\sim 20 \text{ mWm}^{-2}$ . Finally, methane-induced net ozone forcing due to doubling its concentrations relative to present-day under ozone recovery conditions (+++METHANE;  $225.5 \pm 85 \text{ mWm}^{-2}$ ), is not significantly different to that under present-day ODSs concentrations (CLIMATE[CH4-2100] minus +LIGHTNING) or without lightning feedbacks (CLIMATE[CH4-2100]-fLNOx minus CLIMATE). The forcing associated with +++METHANE lies within the latter forcings (i.e.  $50 \text{ mWm}^{-2}$  range). Therefore, we conclude that future ozone forcings due to lightning, ozone recovery and methane



concentrations – presented in Table 3 – are robust, with regard to background conditions.

The fact that global and annual ozone forcings associated with single perturbations are not significantly different with regard to background conditions is perhaps somewhat surprising, given that, for instance, ozone production is sensitive to the relative abundances of volatile organic compounds and NO<sub>x</sub> (e.g. Sillman, 1999). However, while the globally averaged forcing is not significantly affected by the order in which the perturbations are considered, there are significant differences in budget terms (e.g. ozone burden differences due to lightning can be as large as 4.5 ± 1.4 Tg), as well as ozone levels in particular regions of the atmosphere. Therefore, the non-linear additivity of the perturbations is important when considering their impacts on quantities such as ozone profiles and surface air quality (not shown).

## 5 Uncertainties and outlook

We calculate a net ozone radiative forcing of  $417.6 \pm 81 \text{ mWm}^{-2}$  corresponding to the year 2100 compared to present-day, with the one standard deviation uncertainty arising from variability in ozone between the years of the time slice simulations. This variability indicates a ±19 % uncertainty, which is similar to the spread across the ACCMIP ensemble (Stevenson et al., 2013). However, different sources of uncertainty exist in the ozone forcing. Background conditions affect somewhat the resulting ozone forcings (see Sect. 4.4), and therefore add an extra ±2.5 % to the overall uncertainty. Previously, uncertainties arising from the tropopause definition (±3 %), the radiation scheme or forcing calculation (±10 %), and the extent to which clouds and stratospheric temperature adjustment influence ozone forcing (±7 % and ±3 % respectively) have been estimated (Stevenson et al., 2013). Climate feedbacks, land-use change, natural ozone precursor emissions, and future changes in the structure of the tropopause (Wilcox et al., 2012) may introduce at least an additional ±20 % uncertainty (Stevenson et al., 2013). Following Stevenson et al. (2013), we assume that the above individual uncertainties are independent and combine them to estimate an overall uncertainty of ±30 %, which represents the 95 % confidence interval. Note that Skeie et al. (2011) from an independent analysis estimated the same overall uncertainty.



Figure 5 summarises the global and annual net ozone forcing as well as the forcings by driver and region. Overall, our annual global mean best estimate for the net ozone radiative forcing between 2000 and 2100 is  $420 \pm 130 \text{ mWm}^{-2}$ , with tropospheric and stratospheric forcings of  $300 \pm 90 \text{ mWm}^{-2}$  and  $120 \pm 40 \text{ mWm}^{-2}$ , respectively. Current estimates for tropospheric and stratospheric ozone forcings from 1750 to 2011 are  $400 \pm 20 \text{ mWm}^{-2}$  and  $-50 \pm 100 \text{ mWm}^{-2}$ , respectively (Myhre et al., 2013). An increase of 0.5 DU in tropospheric ozone was estimated in Skeie et al. (2011) from 2000 to 2010, and a tropospheric ozone normalized radiative forcing of  $42 \text{ mWm}^{-2} \text{ DU}^{-1}$  calculated from the ACCMIP ensemble (Stevenson et al., 2013). Therefore, we estimate a net ozone forcing of  $750 \pm 230 \text{ mWm}^{-2}$  from 1750 to 2100 based on our simulations, which is the result of the forcings in the troposphere and the stratosphere ( $690 \pm 210 \text{ mWm}^{-2}$  and  $60 \pm 20 \text{ mWm}^{-2}$  respectively). Our tropospheric forcing is within the range estimated from the ACCMIP models of  $620 \pm 190 \text{ mWm}^{-2}$  (Stevenson et al., 2013).

Previous work has shown that NRF is an appropriate tool for estimating annual and global tropospheric forcings derived from changes in tropospheric column ozone, which in turn reduces the multi-model uncertainty (Gauss et al., 2003). The NRF in our analysis of  $43 \text{ mWm}^{-2} \text{ DU}^{-1}$  is similar to that from the ACCMIP models between the 1850s and 2000s, but larger compared to that in Gauss et al. (2003). This supports the future tropospheric ozone forcings and their uncertainties during the 21st century derived from the ACCMIP ensemble (calculated using the NRF), and may be used as a benchmark for individual studies. The net ozone NRF is  $18 \text{ mWm}^{-2} \text{ DU}^{-1}$  (including changes in the stratosphere). The smaller net ozone NRF compared to the tropospheric ozone NRF is mainly caused by the fact that ozone changes in the upper stratosphere have a relatively negligible impact on RF. While this is in agreement with a previous multi-model study (Gauss et al., 2003), their larger value of  $29 \text{ mWm}^{-2} \text{ DU}^{-1}$  is likely associated with their focus on the lower stratosphere only, where ozone is more radiatively efficient than in the upper stratosphere.

Although previous studies have examined key drivers of ozone during the 21st century and future changes are relatively well understood (e.g. Kawase et al., 2011; Banerjee et al., 2014; Banerjee et al., 2016), the resulting forcings have been explored in less detail (e.g. Gauss et al., 2003; Stevenson et al., 2013). Following a process-based approach that includes chemistry-climate feedbacks, we calculate that climate-



only, lightning, ozone recovery and methane emissions contribute respectively  
-10 ± 18 %, 25 ± 19 %, 31 ± 19 %, and 54 ± 20 % to the net ozone RF between 2000  
and 2100 (Table 3 and Fig. 4). Further uncertainties arise from the long-term ozone  
response to methane changes, which could increase the overall tropospheric forcing  
5 by ~15 %. Climate change (including lightning feedbacks) leaves a small tropospheric  
ozone forcing of 64.1 ± 44 mWm<sup>-2</sup>. A subset of eight models from the ACCMIP  
activity shows a small negative but not significant tropospheric forcing of  
-33 ± 42 mWm<sup>-2</sup>, with few models reporting positive forcings (Stevenson et al.,  
2013). The impact of climate change on ozone forcing is surrounded by large  
10 uncertainties, which may be associated with chemistry-climate feedbacks and the lack  
of confidence in the LNO<sub>x</sub> sensitivity to global mean surface temperature, due to  
different parameterizations and the vertical distributions of the emissions (Banerjee et  
al., 2014; Finney et al., 2016), as well as changes in the BDC (Butchart, 2014). For  
example, the climate change-induced net ozone forcing between 2000–2100 –  
15 following the future emission scenario RCP8.5 in an independent CCM – is of the  
same order of magnitude but different sign (-70 mWm<sup>-2</sup>) (Banerjee et al., 2017).  
While they found similar tropospheric ozone forcing of 80 mWm<sup>-2</sup>, their negative  
stratospheric ozone forcing outweighs the latter (-150 mWm<sup>-2</sup>). Methane- and ODSs-  
induced ozone forcings have respectively a substantial contribution from the  
20 stratosphere (~14 %) and the troposphere (~34 %), recently shown in modelling  
studies (Søvde et al., 2011; Shindell et al., 2013; Banerjee et al., 2017). A striking  
result, however, is the contribution of the stratospheric-produced ozone to the net  
forcing of ~30 ± 17 % and ~99 ± 59 % due to methane and ODSs emissions,  
respectively. This reflects the roles that methane plays in stratospheric ozone  
25 chemistry (i.e. particularly in the lower stratosphere), and that ozone recovery  
principally occurs in the stratosphere.

## 6 Summary and conclusions

This study has explored future changes in ozone by the end of the 21st century and the  
30 resulting radiative forcing following a process-based approach, imposing one forcing  
at a time. We have used the RCP8.5 to represent an upper limit on these responses.  
This is a different approach to previous studies, which typically have either explored  
future changes in ozone concentrations or ozone forcing. The methane feedbacks (due



to the changing oxidising capacity of the atmosphere, and due to the long-term tropospheric ozone response) and its forcing have also been accounted for. In addition, non-linearities arising from chemistry-climate interactions have been investigated.

5           The simulated present-day ozone radiative effect is in good agreement with estimates based on observed ozone from TES, particularly in terms of its spatial distribution. However, there are systematic biases: RE is overestimated in the NH and underestimated in the SH, with significant biases in the subtropics. These RE biases are mostly consistent with the biases in tropospheric ozone in current climate models  
10 (Young et al., 2017), although the simulated annual global present-day tropospheric column ozone ( $28.9 \pm 1.5$  DU) is within observed interannual variability of 28.1–34.1 DU (Young et al., 2013). The fact that the biases are apparent in many climate models suggests a common deficiency, and emissions data have been proposed as a likely candidate (Young et al., 2013; Young et al., 2017).

15           Our analysis shows that the ozone radiative forcing arising from climate driven changes is small and not significant ( $63 \pm 76$  mWm<sup>-2</sup>), which is largely the result of the interplay between lightning-produced ozone and enhanced ozone destruction (via increased temperatures and humidity). Higher methane concentrations and reduced ODSs levels also have consequences for ozone forcing in the stratosphere  
20 ( $32 \pm 31$  mWm<sup>-2</sup>) and the troposphere ( $46 \pm 47$  mWm<sup>-2</sup>) respectively. We have demonstrated both the importance of stratospheric-tropospheric interactions and the stratosphere as a key region controlling a large fraction of the tropospheric ozone forcing (i.e. from the source point of view compared to the more common division by recipient-region).

25           Future annual and global tropospheric and stratospheric column ozone changes from year 2000 to 2100 in this set of simulations (7.0 DU and 21.3 DU respectively) are mainly driven by methane and ODSs emissions, respectively (Table S1). These changes lead to a net ozone radiative forcing of  $420 \pm 130$  mWm<sup>-2</sup> compared to present-day, with an overall uncertainty of  $\pm 30$  % (i.e. representing the  
30 95 % confidence interval). Relative to the pre-industrial period (year 1750), our best estimate for the year 2100 net ozone radiative forcing is  $750 \pm 230$  mWm<sup>-2</sup>.



This study highlights the key role of the stratosphere in determining future ozone radiative forcing in spite of the fact that the impacts largely take place in the troposphere. Increasing confidence in present-day observations of the Brewer-Dobson circulation and the stratospheric-tropospheric exchange will therefore play a crucial  
5 role in improving climate models and better constraining ozone radiative forcing. A future study will address the importance of the stratosphere on future air quality commitments, which may better inform emission regulations.

*Acknowledgements.* This work was supported by NERC, under project number  
10 NE/L501736/1. F. Iglesias-Suarez would like to acknowledge NERC for a PhD studentship and thank F. Govantes for hosting him at the Centro Andaluz de Biología del Desarrollo (CABD) while he completed some of this work. WACCM is a component of the Community Earth System Model (CESM), which is supported by the NSF and the Office of Science of the U.S. Department of Energy. Computing  
15 resources were provided by NCAR's Climate Simulation Laboratory, sponsored by the NSF and other agencies. This research was enabled by the computational and storage resources of NCAR's Computational and Information Systems Laboratory (CISL). We thank the NASA JPL TES team for releasing the TES ozone.



## References

- Andrews, D. G., Holton, J. R., and Leovy, C. B.: Middle atmosphere dynamics, International Geophysics Series, Academic press, San Diego, USA, 1987.
- Arblaster et al.: Stratospheric ozone changes and climate, Chapter 4, in: Scientific Assessment of Ozone Depletion: 2014, Global Ozone Research and Monitoring Project, 2014.
- 5 Austin, J., and Wilson, R. J.: Ensemble simulations of the decline and recovery of stratospheric ozone, *J. Geophys. Res.*, 111, 2156-2202, doi:10.1029/2005JD006907, 2006.
- 10 Banerjee, A., Archibald, A. T., Maycock, A. C., Telford, P., Abraham, N. L., Yang, X., Braesicke, P., and Pyle, J. A.: Lightning NO<sub>x</sub>, a key chemistry–climate interaction: impacts of future climate change and consequences for tropospheric oxidising capacity, *Atmos. Chem. Phys.*, 14, 9871-9881, doi:10.5194/acp-14-9871-2014, 2014.
- 15 Banerjee, A., Maycock, A. C., Archibald, A. T., Abraham, N. L., Telford, P., Braesicke, P., and Pyle, J. A.: Drivers of changes in stratospheric and tropospheric ozone between year 2000 and 2100, *Atmos. Chem. Phys.*, 16, 2727-2746, doi:10.5194/acp-16-2727-2016, 2016.
- Banerjee, A., Maycock, A. C., and Pyle, J. A.: Chemical and climatic drivers of radiative forcing due to changes in stratospheric and tropospheric ozone over the 21st century, *Atmos. Chem. Phys. Discuss.*, 2017, 1-19, doi:10.5194/acp-2017-741, 2017.
- 20 Berntsen, T. K., Isaksen, I. S. A., Myhre, G., Fuglestad, J. S., Stordal, F., Larsen, T. A., Freckleton, R. S., and Shine, K. P.: Effects of anthropogenic emissions on tropospheric ozone and its radiative forcing, *J. Geophys. Res.*, 102, 2156-2202, doi:10.1029/97JD02226, 1997.
- 25 Birner, T., and Bönisch, H.: Residual circulation trajectories and transit times into the extratropical lowermost stratosphere, *Atmos. Chem. Phys.*, 11, 817-827, doi:10.5194/acp-11-817-2011, 2011.
- Brasseur, G. P., Schultz, M., Granier, C., Saunio, M., Diehl, T., Botzet, M., Roeckner, E., and Walters, S.: Impact of Climate Change on the Future Chemical Composition of the Global Troposphere, *J. Clim.*, 19, 3932-3951, doi:10.1175/JCLI3832.1, 2006.
- 30 Butchart, N., Cionni, I., Eyring, V., Shepherd, T. G., Waugh, D. W., Akiyoshi, H., Austin, J., Brühl, C., Chipperfield, M. P., Cordero, E., Dameris, M., Deckert, R., Dhomse, S., Frith, S. M., Garcia, R. R., Gettelman, A., Giorgetta, M. A., Kinnison, D. E., Li, F., Mancini, E., McLandress, C., Pawson, S., Pitari, G., Plummer, D. A., Rozanov, E., Sassi, F., Scinocca, J. F., Shibata, K., Steil, B., and Tian, W.: Chemistry–Climate Model Simulations of Twenty-First Century Stratospheric Climate and Circulation Changes, *J. Clim.*, 23, 5349-5374, doi:10.1175/2010JCLI3404.1, 2010.
- 35 40 Butchart, N.: The Brewer-Dobson circulation, *Rev. Geophys.*, 52, 157-184, doi:10.1002/2013RG000448, 2014.



- Calvo, N., Garcia, R. R., and Kinnison, D. E.: Revisiting Southern Hemisphere polar stratospheric temperature trends in WACCM: The role of dynamical forcing, *Geophys. Res. Lett.*, 44, 2017GL072792, doi:10.1002/2017GL072792, 2017.
- 5 Chipperfield, M. P., Bekki, S., Dhomse, S., Harris, N. R. P., Hassler, B., Hossaini, R., Steinbrecht, W., Thiéblemont, R., and Weber, M.: Detecting recovery of the stratospheric ozone layer, *Nature*, 549, 211-218, doi:10.1038/nature23681, 2017.
- Collins, W. J., Derwent, R. G., Garnier, B., Johnson, C. E., Sanderson, M. G., and Stevenson, D. S.: Effect of stratosphere-troposphere exchange on the future tropospheric ozone trend, *J. Geophys. Res.*, 108, 8528, doi:10.1029/2002JD002617, 10 2003.
- Dahlmann, K., Grewe, V., Ponater, M., and Matthes, S.: Quantifying the contributions of individual NO<sub>x</sub> sources to the trend in ozone radiative forcing, *Atmos. Environ.*, 45, 2860-2868, doi:10.1016/j.atmosenv.2011.02.071, 2011.
- 15 Emmons, L. K., Walters, S., Hess, P. G., Lamarque, J. F., Pfister, G. G., Fillmore, D., Granier, C., Guenther, A., Kinnison, D., Laepple, T., Orlando, J., Tie, X., Tyndall, G., Wiedinmyer, C., Baughcum, S. L., and Kloster, S.: Description and evaluation of the Model for Ozone and Related chemical Tracers, version 4 (MOZART-4), *Geosci. Model Dev.*, 3, 43-67, doi:10.5194/gmd-3-43-2010, 2010.
- 20 Engel, A., Mobius, T., Bonisch, H., Schmidt, U., Heinz, R., Levin, I., Atlas, E., Aoki, S., Nakazawa, T., Sugawara, S., Moore, F., Hurst, D., Elkins, J., Schauffler, S., Andrews, A., and Boering, K.: Age of stratospheric air unchanged within uncertainties over the past 30 years, *Nature Geosci.*, 2, 28-31, doi:10.1038/ngeo388, 2009.
- 25 Eyring, V., Cionni, I., Bodeker, G. E., Charlton-Perez, A. J., Kinnison, D. E., Scinocca, J. F., Waugh, D. W., Akiyoshi, H., Bekki, S., Chipperfield, M. P., Dameris, M., Dhomse, S., Frith, S. M., Garny, H., Gettelman, A., Kubin, A., Langematz, U., Mancini, E., Marchand, M., Nakamura, T., Oman, L. D., Pawson, S., Pitari, G., Plummer, D. A., Rozanov, E., Shepherd, T. G., Shibata, K., Tian, W., Braesicke, P., Hardiman, S. C., Lamarque, J. F., Morgenstern, O., Pyle, J. A., Smale, D., and Yamashita, Y.: Multi-model assessment of stratospheric ozone return dates and ozone recovery in CCMVal-2 models, *Atmos. Chem. Phys.*, 10, 9451-9472, doi:10.5194/acp-10-9451-2010, 2010.
- 35 Eyring, V., Lamarque, J.-F., Hess, P., Arfeuille, F., Bowman, K., Chipperfield, M. P., Duncan, B., Fiore, A., Gettelman, A., Giorgetta, M. a., Granier, C., Hegglin, M. I., Kinnison, D., Kunze, M., Langematz, U., Luo, B., Martin, R., Matthes, K., Newman, P. a., Peter, T., Robock, A., Ryerson, T., Saiz-Lopez, A., Salawitch, R., Schultz, M., Shepherd, T. G., Shindell, D., Stähelin, J., Tegtmeier, S., Thomason, L., Tilmes, S., Vernier, J.-P., Waugh, D. W., and Young, P. J.: Overview of IGAC/SPARC Chemistry-Climate Model Initiative (CCMI) Community Simulations in Support of Upcoming Ozone and Climate Assessments, WMO-WRCP, Geneva, Switzerland, 48-40 66, 2013.
- 45 Finney, D. L., Doherty, R. M., Wild, O., Young, P. J., and Butler, A.: Response of lightning NO<sub>x</sub> emissions and ozone production to climate change: Insights from the Atmospheric Chemistry and Climate Model Intercomparison Project, *Geophys. Res. Lett.*, 43, 2016GL068825, doi:10.1002/2016GL068825, 2016.





- 5 Fiore, A. M., Dentener, F. J., Wild, O., Cuvelier, C., Schultz, M. G., Hess, P., Textor, C., Schulz, M., Doherty, R. M., Horowitz, L. W., MacKenzie, I. A., Sanderson, M. G., Shindell, D. T., Stevenson, D. S., Szopa, S., Van Dingenen, R., Zeng, G., Atherton, C., Bergmann, D., Bey, I., Carmichael, G., Collins, W. J., Duncan, B. N., Faluvegi, G., Folberth, G., Gauss, M., Gong, S., Hauglustaine, D., Holloway, T., Isaksen, I. S. A., Jacob, D. J., Jonson, J. E., Kaminski, J. W., Keating, T. J., Lupu, A., Marmer, E., Montanaro, V., Park, R. J., Pitari, G., Pringle, K. J., Pyle, J. A., Schroeder, S., Vivanco, M. G., Wind, P., Wojcik, G., Wu, S., and Zuber, A.: Multimodel estimates of intercontinental source-receptor relationships for ozone  
10 pollution, *J. Geophys. Res.*, 114, D04301, doi:10.1029/2008JD010816, 2009.
- Fleming, E. L., Jackman, C. H., Stolarski, R. S., and Douglass, A. R.: A model study of the impact of source gas changes on the stratosphere for 1850–2100, *Atmos. Chem. Phys.*, 11, 8515–8541, doi:10.5194/acp-11-8515-2011, 2011.
- 15 Forster, P. M., and Shine, K. P.: Radiative forcing and temperature trends from stratospheric ozone changes, *J. Geophys. Res.*, 102, 10841–10855, doi:10.1029/96JD03510, 1997.
- Fuglestedt, J. S., Berntsen, T. K., Isaksen, I. S. A., Mao, H., Liang, X.-Z., and Wang, W.-C.: Climatic forcing of nitrogen oxides through changes in tropospheric ozone and methane; global 3D model studies, *Atmos. Environ.*, 33, 961–977,  
20 doi:10.1016/S1352-2310(98)00217-9, 1999.
- Galloway, J. N., Dentener, F. J., Capone, D. G., Boyer, E. W., Howarth, R. W., Seitzinger, S. P., Asner, G. P., Cleveland, C. C., Green, P. A., Holland, E. A., Karl, D. M., Michaels, A. F., Porter, J. H., Townsend, A. R., and Vöosmarty, C. J.: Nitrogen Cycles: Past, Present, and Future, *Biogeochemistry*, 70, 153–226,  
25 doi:10.1007/s10533-004-0370-0, 2004.
- Garcia, R. R., and Randel, W. J.: Acceleration of the Brewer–Dobson Circulation due to Increases in Greenhouse Gases, *J. Atmos. Sci.*, 65, 2731–2739, doi:10.1175/2008JAS2712.1, 2008.
- 30 Garcia, R. R., Smith, A. K., Kinnison, D. E., Cámara, Á. d. I., and Murphy, D. J.: Modification of the Gravity Wave Parameterization in the Whole Atmosphere Community Climate Model: Motivation and Results, *J. Atmos. Sci.*, 74, 275–291, doi:10.1175/JAS-D-16-0104.1, 2017.
- Gauss, M., Myhre, G., Pitari, G., Prather, M. J., Isaksen, I. S. A., Berntsen, T. K., Brasseur, G. P., Dentener, F. J., Derwent, R. G., Hauglustaine, D. A., Horowitz, L. W., Jacob, D. J., Johnson, M., Law, K. S., Mickley, L. J., Müller, J. F., Plantevin, P. H., Pyle, J. A., Rogers, H. L., Stevenson, D. S., Sundet, J. K., van Weele, M., and Wild, O.: Radiative forcing in the 21st century due to ozone changes in the troposphere and the lower stratosphere, *J. Geophys. Res.*, 108, 4292, doi:10.1029/2002JD002624, 2003.
- 40 Guenther, A. B., Jiang, X., Heald, C. L., Sakulyanontvittaya, T., Duhl, T., Emmons, L. K., and Wang, X.: The Model of Emissions of Gases and Aerosols from Nature version 2.1 (MEGAN2.1): an extended and updated framework for modeling biogenic emissions, *Geosci. Model Dev.*, 5, 1471–1492, doi:10.5194/gmd-5-1471-2012, 2012.
- 45 Haigh, J. D., and Pyle, J. A.: Ozone perturbation experiments in a two-dimensional circulation model, *Quart. J. Roy. Meteor. Soc.*, 108, 551–574, doi:10.1002/qj.49710845705, 1982.



- Hardiman, S. C., Butchart, N., and Calvo, N.: The morphology of the Brewer–Dobson circulation and its response to climate change in CMIP5 simulations, *Quart. J. Roy. Meteor. Soc.*, 140, 1958-1965, doi:10.1002/qj.2258, 2014.
- 5 Hegglin, M. I., and Shepherd, T. G.: Large climate-induced changes in ultraviolet index and stratosphere-to-troposphere ozone flux, *Nature Geosci.*, 2, 687-691, doi:10.1038/ngeo604, 2009.
- Hegglin, M. I., Plummer, D. A., Shepherd, T. G., Scinocca, J. F., Anderson, J., Froidevaux, L., Funke, B., Hurst, D., Rozanov, A., Urban, J., von Clarmann, T., Walker, K. A., Wang, H. J., Tegtmeier, S., and Weigel, K.: Vertical structure of stratospheric water vapour trends derived from merged satellite data, *Nature Geosci.*, 7, 768-776, doi:10.1038/ngeo2236, 2014.
- 10 Holmes, C. D., Prather, M. J., Søvde, O. A., and Myhre, G.: Future methane, hydroxyl, and their uncertainties: key climate and emission parameters for future predictions, *Atmos. Chem. Phys.*, 13, 285-302, doi:10.5194/acp-13-285-2013, 2013.
- 15 Iglesias-Suarez, F., Young, P. J., and Wild, O.: Stratospheric ozone change and related climate impacts over 1850–2100 as modelled by the ACCMIP ensemble, *Atmos. Chem. Phys.*, 16, 343-363, doi:10.5194/acp-16-343-2016, 2016.
- Jacob, D.: Introduction to atmospheric chemistry, Princeton University Press, Princeton, USA, 1999.
- 20 Johnson, C. E., Stevenson, D. S., Collins, W. J., and Derwent, R. G.: Role of climate feedback on methane and ozone studied with a Coupled Ocean-Atmosphere-Chemistry Model, *Geophys. Res. Lett.*, 28, 1723-1726, doi:10.1029/2000GL011996, 2001.
- Kawase, H., Nagashima, T., Sudo, K., and Nozawa, T.: Future changes in tropospheric ozone under Representative Concentration Pathways (RCPs), *Geophys. Res. Lett.*, 38, 1944-8007, doi:10.1029/2010gl046402, 2011.
- 25 Kinnison, D. E., Brasseur, G. P., Walters, S., Garcia, R. R., Marsh, D. R., Sassi, F., Harvey, V. L., Randall, C. E., Emmons, L., Lamarque, J. F., Hess, P., Orlando, J. J., Tie, X. X., Randel, W., Pan, L. L., Gettelman, A., Granier, C., Diehl, T., Niemeier, U., and Simmons, A. J.: Sensitivity of chemical tracers to meteorological parameters in the MOZART-3 chemical transport model, *J. Geophys. Res.*, 112, 2156-2202, doi:10.1029/2006JD007879, 2007.
- 30 Lacis, A. A., Wuebbles, D. J., and Logan, J. A.: Radiative forcing of climate by changes in the vertical distribution of ozone, *J. Geophys. Res.*, 95, 9971-9981, doi:10.1029/JD095iD07p09971, 1990.
- 35 Lamarque, J. F., Emmons, L. K., Hess, P. G., Kinnison, D. E., Tilmes, S., Vitt, F., Heald, C. L., Holland, E. A., Lauritzen, P. H., Neu, J., Orlando, J. J., Rasch, P. J., and Tyndall, G. K.: CAM-chem: description and evaluation of interactive atmospheric chemistry in the Community Earth System Model, *Geosci. Model Dev.*, 5, 369-411, doi:10.5194/gmd-5-369-2012, 2012.
- 40 Liaskos, C. E., Allen, D. J., and Pickering, K. E.: Sensitivity of tropical tropospheric composition to lightning NO<sub>x</sub> production as determined by replay simulations with GEOS-5, *J. Geophys. Res.*, 120, 2014JD022987, doi:10.1002/2014JD022987, 2015.



- Marsh, D. R., Mills, M. J., Kinnison, D. E., Lamarque, J.-F., Calvo, N., and Polvani, L. M.: Climate Change from 1850 to 2005 Simulated in CESM1(WACCM), *J. Clim.*, 26, 7372-7391, doi:10.1175/JCLI-D-12-00558.1, 2013.
- 5 Meinshausen, M., Smith, S. J., Calvin, K., Daniel, J. S., Kainuma, M. L. T., Lamarque, J. F., Matsumoto, K., Montzka, S. A., Raper, S. C. B., Riahi, K., Thomson, A., Velders, G. J. M., and Vuuren, D. P. P.: The RCP greenhouse gas concentrations and their extensions from 1765 to 2300, *Clim. Change*, 109, 213-241, doi:10.1007/s10584-011-0156-z, 2011.
- 10 Morgenstern, O., Zeng, G., Luke Abraham, N., Telford, P. J., Braesicke, P., Pyle, J. A., Hardiman, S. C., O'Connor, F. M., and Johnson, C. E.: Impacts of climate change, ozone recovery, and increasing methane on surface ozone and the tropospheric oxidizing capacity, *J. Geophys. Res.*, 118, 1028-1041, doi:10.1029/2012JD018382, 2013.
- 15 Morgenstern, O., Hegglin, M. I., Rozanov, E., O'Connor, F. M., Abraham, N. L., Akiyoshi, H., Archibald, A. T., Bekki, S., Butchart, N., Chipperfield, M. P., Deushi, M., Dhomse, S. S., Garcia, R. R., Hardiman, S. C., Horowitz, L. W., Jöckel, P., Josse, B., Kinnison, D., Lin, M., Mancini, E., Manyin, M. E., Marchand, M., Marécal, V., Michou, M., Oman, L. D., Pitari, G., Plummer, D. A., Revell, L. E., Saint-Martin, D., Schofield, R., Stenke, A., Stone, K., Sudo, K., Tanaka, T. Y., Tilmes, S., Yamashita, Y., Yoshida, K., and Zeng, G.: Review of the global models used within phase 1 of the Chemistry–Climate Model Initiative (CCMI), *Geosci. Model Dev.*, 10, 639-671, doi:10.5194/gmd-10-639-2017, 2017.
- 20 Myhre, G., Shindell, D., Breion, F.-M., Collins, W., Fuglestedt, J., Huang, J., Koch, D., Lamarque, J.-F., Lee, D., Mendoza, B., Nakajima, T., Robock, A., Stephens, G., Takemura, T., and Zhang, H.: Anthropogenic and Natural Radiative Forcing, in: *Climate Change: The Physical Science Basis. Contribution of Working Group I to the Fifth Assessment Report of the Intergovernmental Panel on Climate Change*, [Stocker, T. F., Qin, D., Plattner, G.-K., Tignor, M., Allen, S. K., Boschung, J., Nauels, A., Xia, Y., Bex, V., and Midgley, P. M. (eds)], Cambridge University Press, Cambridge, United Kingdom and New York, NY, USA, 659–740, 2013.
- 30 Oberländer, S., Langematz, U., and Meul, S.: Unraveling impact factors for future changes in the Brewer-Dobson circulation, *J. Geophys. Res.*, 118, 10,296-210,312, doi:10.1002/jgrd.50775, 2013.
- 35 Osterman, G. B., Kulawik, S. S., Worden, H. M., Richards, N. A. D., Fisher, B. M., Eldering, A., Shephard, M. W., Froidevaux, L., Labow, G., Luo, M., Herman, R. L., Bowman, K. W., and Thompson, A. M.: Validation of Tropospheric Emission Spectrometer (TES) measurements of the total, stratospheric, and tropospheric column abundance of ozone, *J. Geophys. Res.*, 113, D15S16, doi:10.1029/2007JD008801, 2008.
- 40 Ploeger, F., Riese, M., Haenel, F., Konopka, P., Müller, R., and Stiller, G.: Variability of stratospheric mean age of air and of the local effects of residual circulation and eddy mixing, *J. Geophys. Res.*, 120, 2014JD022468, 10.1002/2014JD022468, 2015.
- 45 Portmann, R. W., and Solomon, S.: Indirect radiative forcing of the ozone layer during the 21st century, *Geophys. Res. Lett.*, 34, L02813, doi:10.1029/2006GL028252, 2007.



- Prather M., Ehalt, D., Dentener, F., Derwent, R., Dlugokencky, E., Holland, E., Isaksen, I., Katima, J., Kirchhoff, V., Matson, P., Midgley, P., Wang, M., Atmospheric chemistry and greenhouse gases. In: Climate change: The scientific basis. Contribution of Working Group I to the Third Assessment Report of the Intergovernmental Panel on Climate Change, [Houghton J. T., Ding, Y., Griggs, D. J., Noguera, M., van der Linden, P. J., Dai, X., Maskell, K., Johnson, C. A. (eds)], Cambridge University Press, Cambridge, UK, 2001.
- 5
- Prather, M. J., Zhu, X., Tang, Q., Hsu, J., and Neu, J. L.: An atmospheric chemist in search of the tropopause, *J. Geophys. Res.*, 116, 2156-2202, doi:10.1029/2010JD014939, 2011.
- 10
- Prather, M. J., Holmes, C. D., and Hsu, J.: Reactive greenhouse gas scenarios: Systematic exploration of uncertainties and the role of atmospheric chemistry, *Geophys. Res. Lett.*, 39, L09803, doi:10.1029/2012GL051440, 2012.
- Price, J. D., and Vaughan, G.: The potential for stratosphere-troposphere exchange in cut-off-low systems, *Quart. J. Roy. Meteor. Soc.*, 119, 343-365, doi:10.1002/qj.49711951007, 1993.
- 15
- Randeniya, L. K., Vohralik, P. F., and Plumb, I. C.: Stratospheric ozone depletion at northern mid latitudes in the 21st century: The importance of future concentrations of greenhouse gases nitrous oxide and methane, *Geophys. Res. Lett.*, 29, 10-11-10-14, doi:10.1029/2001GL014295, 2002.
- 20
- Rap, A., Richards, N. A. D., Forster, P. M., Monks, S. A., Arnold, S. R., and Chipperfield, M. P.: Satellite constraint on the tropospheric ozone radiative effect, *Geophys. Res. Lett.*, 42, 2015GL064037, doi:10.1002/2015GL064037, 2015.
- Ray, E. A., Moore, F. L., Rosenlof, K. H., Davis, S. M., Sweeney, C., Tans, P., Wang, T., Elkins, J. W., Bönisch, H., Engel, A., Sugawara, S., Nakazawa, T., and Aoki, S.: Improving stratospheric transport trend analysis based on SF6 and CO2 measurements, *J. Geophys. Res.*, 119, 2014JD021802, doi:10.1002/2014JD021802, 2014.
- 25
- Revell, L. E., Bodeker, G. E., Smale, D., Lehmann, R., Huck, P. E., Williamson, B. E., Rozanov, E., and Struthers, H.: The effectiveness of N2O in depleting stratospheric ozone, *Geophys. Res. Lett.*, 39, L15806, doi:10.1029/2012GL052143, 2012.
- 30
- Riese, M., Ploeger, F., Rap, A., Vogel, B., Konopka, P., Dameris, M., and Forster, P.: Impact of uncertainties in atmospheric mixing on simulated UTLS composition and related radiative effects, *J. Geophys. Res.*, 117, D16305, doi:10.1029/2012JD017751, 2012.
- 35
- Roelofs, G.-J., and Lelieveld, J.: Model study of the influence of cross-tropopause O3 transports on tropospheric O3 levels, *Tellus, Ser. B*, 49, 38-55, doi:10.3402/tellusb.v49i1.15949, 1997.
- Rosenfield, J. E., Douglass, A. R., and Considine, D. B.: The impact of increasing carbon dioxide on ozone recovery, *J. Geophys. Res.*, 107, ACH 7-1-ACH 7-9, doi:10.1029/2001JD000824, 2002.
- 40
- Schumann, U., and Huntrieser, H.: The global lightning-induced nitrogen oxides source, *Atmos. Chem. Phys.*, 7, 3823-3907, doi:10.5194/acp-7-3823-2007, 2007.



- Shindell, D., Faluvegi, G., Nazarenko, L., Bowman, K., Lamarque, J. F., Voulgarakis, A., Schmidt, G. A., Pechony, O., and Ruedy, R.: Attribution of historical ozone forcing to anthropogenic emissions, *Nature Clim. Change*, 3, 567-570, 2013.
- 5 Sillman, S.: The relation between ozone, NO<sub>x</sub> and hydrocarbons in urban and polluted rural environments, *Atmos. Environ.*, 33, 1821-1845, doi:10.1016/S1352-2310(98)00345-8, 1999.
- Skeie, R. B., Berntsen, T. K., Myhre, G., Tanaka, K., Kvalevåg, M. M., and Hoyle, C. R.: Anthropogenic radiative forcing time series from pre-industrial times until 2010, *Atmos. Chem. Phys.*, 11, 11827-11857, doi:10.5194/acp-11-11827-2011, 2011.
- 10 Solomon, S., Kinnison, D., Bandoro, J., and Garcia, R.: Simulation of polar ozone depletion: An update, *J. Geophys. Res.*, 120, 2015JD023365, doi:10.1002/2015JD023365, 2015.
- Søvde, O. A., Hoyle, C. R., Myhre, G., and Isaksen, I. S. A.: The HNO<sub>3</sub> forming branch of the HO<sub>2</sub> + NO reaction: pre-industrial-to-present trends in atmospheric species and radiative forcings, *Atmos. Chem. Phys.*, 11, 8929-8943, doi:10.5194/acp-11-8929-2011, 2011.
- 15 Squire, O. J., Archibald, A. T., Abraham, N. L., Beerling, D. J., Hewitt, C. N., Lathièrre, J., Pike, R. C., Telford, P. J., and Pyle, J. A.: Influence of future climate and cropland expansion on isoprene emissions and tropospheric ozone, *Atmos. Chem. Phys.*, 14, 1011-1024, doi:10.5194/acp-14-1011-2014, 2014.
- 20 Stenke, A., and Grewe, V.: Simulation of stratospheric water vapor trends: impact on stratospheric ozone chemistry, *Atmos. Chem. Phys.*, 5, 1257-1272, doi:10.5194/acp-5-1257-2005, 2005.
- 25 Stevenson, D. S., Dentener, F. J., Schultz, M. G., Ellingsen, K., van Noije, T. P. C., Wild, O., Zeng, G., Amann, M., Atherton, C. S., Bell, N., Bergmann, D. J., Bey, I., Butler, T., Cofala, J., Collins, W. J., Derwent, R. G., Doherty, R. M., Drevet, J., Eskes, H. J., Fiore, A. M., Gauss, M., Hauglustaine, D. A., Horowitz, L. W., Isaksen, I. S. A., Krol, M. C., Lamarque, J. F., Lawrence, M. G., Montanaro, V., Müller, J. F., Pitari, G., Prather, M. J., Pyle, J. A., Rast, S., Rodriguez, J. M., Sanderson, M. G.,
- 30 Savage, N. H., Shindell, D. T., Strahan, S. E., Sudo, K., and Szopa, S.: Multimodel ensemble simulations of present-day and near-future tropospheric ozone, *J. Geophys. Res.*, 111, D08301, doi:10.1029/2005JD006338, 2006.
- 35 Stevenson, D. S., Young, P. J., Naik, V., Lamarque, J. F., Shindell, D. T., Voulgarakis, A., Skeie, R. B., Dalsoren, S. B., Myhre, G., Berntsen, T. K., Folberth, G. A., Rumbold, S. T., Collins, W. J., MacKenzie, I. A., Doherty, R. M., Zeng, G., van Noije, T. P. C., Strunk, A., Bergmann, D., Cameron-Smith, P., Plummer, D. A., Strode, S. A., Horowitz, L., Lee, Y. H., Szopa, S., Sudo, K., Nagashima, T., Josse, B., Cionni, I., Righi, M., Eyring, V., Conley, A., Bowman, K. W., Wild, O., and Archibald, A.: Tropospheric ozone changes, radiative forcing and attribution to emissions in the Atmospheric Chemistry and Climate Model Intercomparison Project (ACCMIP), *Atmos. Chem. Phys.*, 13, 3063-3085, doi:10.5194/acp-13-3063-2013, 2013.
- 40 Stiller, G. P., Fierli, F., Ploeger, F., Cagnazzo, C., Funke, B., Haenel, F. J., Reddman, T., Riese, M., and von Clarmann, T.: Shift of subtropical transport barriers explains observed hemispheric asymmetry of decadal trends of age of air, *Atmos. Chem. Phys.*, 17, 11177-11192, doi:10.5194/acp-17-11177-2017, 2017.
- 45



- Sudo, K., Takahashi, M., and Akimoto, H.: Future changes in stratosphere-troposphere exchange and their impacts on future tropospheric ozone simulations, *Geophys. Res. Lett.*, 30, 2256, doi:10.1029/2003GL018526, 2003.
- 5 Tilmes, S., Lamarque, J. F., Emmons, L. K., Kinnison, D. E., Ma, P. L., Liu, X., Ghan, S., Bardeen, C., Arnold, S., Deeter, M., Vitt, F., Ryerson, T., Elkins, J. W., Moore, F., Spackman, J. R., and Val Martin, M.: Description and evaluation of tropospheric chemistry and aerosols in the Community Earth System Model (CESM1.2), *Geosci. Model Dev.*, 8, 1395-1426, doi:10.5194/gmd-8-1395-2015, 2015.
- 10 Tilmes, S., Lamarque, J. F., Emmons, L. K., Kinnison, D. E., Marsh, D., Garcia, R. R., Smith, A. K., Neely, R. R., Conley, A., Vitt, F., Val Martin, M., Tanimoto, H., Simpson, I., Blake, D. R., and Blake, N.: Representation of the Community Earth System Model (CESM1) CAM4-chem within the Chemistry-Climate Model Initiative (CCMI), *Geosci. Model Dev.*, 9, 1853-1890, doi:10.5194/gmd-9-1853-2016, 2016.
- 15 UNEP: Environmental effects of ozone depletion and its interaction with climate change: 2014 assessment, United Nations Environment Programme (UNEP), Nairobi, 2015.
- Val Martin, M., Heald, C. L., and Arnold, S. R.: Coupling dry deposition to vegetation phenology in the Community Earth System Model: Implications for the simulation of surface O<sub>3</sub>, *Geophys. Res. Lett.*, 41, 2988-2996, doi:10.1002/2014GL059651, 2014.
- 20 van Vuuren, Detlef, P., Edmonds, J., Kainuma, M., Riahi, K., Thomson, A., Hibbard, K., Hurtt, G., Kram, T., Krey, V., Lamarque, J.-F., Masui, T., Meinshausen, M., Nakicenovic, N., Smith, S., and Rose, S.: The representative concentration pathways: an overview, *Clim. Change*, 109, 5-31, doi:10.1007/s10584-011-0148-z, 2011.
- 25 Voulgarakis, A., Naik, V., Lamarque, J. F., Shindell, D. T., Young, P. J., Prather, M. J., Wild, O., Field, R. D., Bergmann, D., Cameron-Smith, P., Cionni, I., Collins, W. J., Dalsören, S. B., Doherty, R. M., Eyring, V., Faluvegi, G., Folberth, G. A., Horowitz, L. W., Josse, B., MacKenzie, I. A., Nagashima, T., Plummer, D. A., Righi, M., Rumbold, S. T., Stevenson, D. S., Stode, S. A., Sudo, K., Szopa, S., and Zeng, G.: Analysis of present day and future OH and methane lifetime in the ACCMIP simulations, *Atmos. Chem. Phys.*, 13, 2563-2587, doi:10.5194/acp-13-2563-2013, 2013.
- 30 Wegner, T., Kinnison, D. E., Garcia, R. R., and Solomon, S.: Simulation of polar stratospheric clouds in the specified dynamics version of the whole atmosphere community climate model, *J. Geophys. Res.*, 118, 4991-5002, doi:10.1002/jgrd.50415, 2013.
- Wilcox, L. J., Charlton-Perez, A. J., and Gray, L. J.: Trends in Austral jet position in ensembles of high- and low-top CMIP5 models, *J. Geophys. Res.*, 117, D13115, doi:10.1029/2012JD017597, 2012.
- 40 Wild, O., and Prather, M. J.: Excitation of the primary tropospheric chemical mode in a global three-dimensional model, *J. Geophys. Res.*, 105, 24647-24660, 10.1029/2000JD900399, 2000.
- 45 Wild, O.: Modelling the global tropospheric ozone budget: exploring the variability in current models, *Atmos. Chem. Phys.*, 7, 2643-2660, doi:10.5194/acp-7-2643-2007, 2007.



- Williams, E. R.: Lightning and climate: A review, *Atmospheric Research*, 76, 272-287, doi:10.1016/j.atmosres.2004.11.014, 2005.
- WMO: Scientific Assessment of Ozone Depletion: 2010, World Meteorological Organization, Geneva, Switzerland, 516 pp., 2011.
- 5 WMO: Scientific Assessment of Ozone Depletion: 2014, World Meteorological Organization, Global Ozone Research and Monitoring Project, Geneva, Switzerland, 2014.
- Worden, H. M., Bowman, K. W., Kulawik, S. S., and Aghedo, A. M.: Sensitivity of outgoing longwave radiative flux to the global vertical distribution of ozone characterized by instantaneous radiative kernels from Aura-TES, *J. Geophys. Res.*, 116, D14115, doi:10.1029/2010JD015101, 2011.
- Young, P. J., Archibald, A. T., Bowman, K. W., Lamarque, J. F., Naik, V., Stevenson, D. S., Tilmes, S., Voulgarakis, A., Wild, O., Bergmann, D., Cameron-Smith, P., Cionni, I., Collins, W. J., Dalsoren, S. B., Doherty, R. M., Eyring, V., Faluvegi, G., Horowitz, L. W., Josse, B., Lee, Y. H., MacKenzie, I. A., Nagashima, T., Plummer, D. A., Righi, M., Rumbold, S. T., Skeie, R. B., Shindell, D. T., Strode, S. A., Sudo, K., Szopa, S., and Zeng, G.: Pre-industrial to end 21st century projections of tropospheric ozone from the Atmospheric Chemistry and Climate Model Intercomparison Project (ACCMIP), *Atmos. Chem. Phys.*, 13, 2063-2090, doi:10.5194/acp-13-2063-2013, 2013.
- 15 Young, P. J., Naik, V., Fiore, A. M., Gaudel, A., Guo, J., Lin, M. Y., Neu, J., Parrish, D. D., Rieder, H. E., Schnell, J. L., Tilmes, S., Wild, O., Zhang, L., Brandt, J., Delcloo, A., Doherty, R. M., Geels, C., Hegglin, M. I., Hu, L., Im, U., Kumar, R., Luhar, A., Murray, L., Plummer, D., Rodriguez, J., Saiz-Lopez, A., Schultz, M. G.,
- 25 Woodhouse, M., Zeng, G., Ziemke, J., Assessment of global-scale model performance for global and regional ozone distributions, variability, and trends, in: *Tropospheric Ozone Assessment Report*, submitted to *Elementa Science of the Anthropocene*, 2017.
- Zeng, G., and Pyle, J. A.: Changes in tropospheric ozone between 2000 and 2100 modeled in a chemistry-climate model, *Geophys. Res. Lett.*, 30, 1392, doi:10.1029/2002GL016708, 2003.
- 30 Zeng, G., Pyle, J. A., and Young, P. J.: Impact of climate change on tropospheric ozone and its global budgets, *Atmos. Chem. Phys.*, 8, 369-387, doi:10.5194/acp-8-369-2008, 2008.
- 35 Zeng, G., Morgenstern, O., Braesicke, P., and Pyle, J. A.: Impact of stratospheric ozone recovery on tropospheric ozone and its budget, *Geophys. Res. Lett.*, 37, L09805, doi:10.1029/2010GL042812, 2010.
- Zhang, H., Wu, S., Huang, Y., and Wang, Y.: Effects of stratospheric ozone recovery on photochemistry and ozone air quality in the troposphere, *Atmos. Chem. Phys.*, 14, 4079-4086, doi:10.5194/acp-14-4079-2014, 2014.
- 40



Table 1. Summary of the model simulations

Simulation	Climate <sup>1</sup>	ODSs <sup>2</sup>	CH <sub>4</sub> <sup>3</sup>
CNTRL	2000	2000	2000
CLIMATE	2100 (fLNOx) <sup>4</sup>	2000	2000
+LIGHTNING	2100	2000	2000
++O3-RECOVERY	2100	2100	2000
+++METHANE	2100	2100	2100
CNTRL+fLNOx	2000 (fLNOx) <sup>4</sup>	2000	2000

<sup>1</sup> Climate (SSTs, sea ice, CO<sub>2</sub> and N<sub>2</sub>O, if not otherwise specified).

<sup>2</sup> Relative to CNTRL, ++O3-RECOVERY simulation is driven by ODSs boundary conditions of -63.2% (2.156 ppbv) total chlorine, -35.7% (8.1 pptv) total bromine and -67.6% (1.376 ppbv) total fluorine.

<sup>3</sup> Relative to CNTRL, +++METHANE simulation is driven by CH<sub>4</sub> boundary conditions of 214.2 % (3744 ppbv).

<sup>4</sup> Offline lightning-induced NO<sub>x</sub> emissions imposed by applying a monthly mean climatology of the CNTRL simulation.

5





**Table 2.** Tropospheric ozone budget, including: Ozone production (P) and loss (L) terms are based on the gas-phase reaction rates of the O<sub>x</sub> family (O<sub>3</sub>, O, O<sub>1</sub>D and NO<sub>2</sub>); Net chemical production of ozone is defined as the residual of the production and loss terms (N = P – L); Dry deposition of ozone (D) term; Stratospheric-Tropospheric exchange (S; i.e. influx from the stratosphere) term is the residual of the dry deposition and net chemistry production terms (S = D – N); Ozone burden (B) term; Ozone and methane lifetimes ( $\tau_{O_3}$ ,  $\tau_{CH_4}$  respectively) is the ratio between the burden and total losses ( $\tau$  = burden / total loss);  $\tau_{CH_4}$  includes loss with respect to OH and adjusted for soil uptake (160 years) and stratospheric sink (120 years) (Prather et al., 2012); Burden for the stratospheric ozone tracer ( $B_{O_3S}$ ) after corrected to include dry deposition (not shown).

Simulation	P (Tg yr <sup>-1</sup> )	L (Tg yr <sup>-1</sup> )	N (Tg yr <sup>-1</sup> )	D (Tg yr <sup>-1</sup> )	S (Tg yr <sup>-1</sup> )	B (Tg)	$\tau_{O_3}$ (years)	$\tau_{CH_4}$ (years)	$B_{O_3S}$ (Tg)
ACCENT (year 2000)	5110 ± 606	4668 ± 727	442 ± 309	1003 ± 200	552 ± 168	344 ± 39	22.3 ± 2.0	8.7 ± 1.3	----
ACCMIP (year 2000)	4877 ± 853	4260 ± 645	618 ± 275	1094 ± 264	477 ± 97	337 ± 23	23.4 ± 2.2	8.5 ± 1.1	----
CNTRL	4678	4195	483	881	398	318	22.9	7.2	123
CLIMATE	5111	4809	302	811	510	309	20.1	6.9	119
+LIGHTNING	5378	5057	322	833	511	329	20.4	6.6	138
++O <sub>3</sub> -RECOVERY	5303	5058	245	855	610	337	20.8	6.6	131
+++METHANE	6072	5759	313	979	666	378	20.5	8.3	138
CNTRL+HNO <sub>x</sub>	4648	4169	479	878	399	313	22.7	7.2	121



Table 3. Global and annual mean ozone RF and the standard deviation<sup>a</sup> ( $\text{mWm}^{-2}$ ) by driver and region, relative to CNTRL (year 2000).

	Whole-atmosphere	Region		Source		CH <sub>4</sub> <sup>b</sup>
		Tropo.	Strat.	Tropo.	Strat.	Tropo.
CLIMATE	$-41.3 \pm 75$	$-40.4 \pm 43$	$-0.8 \pm 27$	$-19.8 \pm 22$	$-21.4 \pm 48$	-7.7
+LIGHTNING	$104.2 \pm 79$	$104.5 \pm 45$	$-0.3 \pm 29$	$79.4 \pm 35$	$24.8 \pm 39$	-11.3
++O <sub>3</sub> -RECOVERY	$129.2 \pm 81$	$45.9 \pm 47$	$83.2 \pm 30$	$0.8 \pm 0.7$	$128.3 \pm 76$	1.9
+++METHANE	$225.5 \pm 85$	$193.1 \pm 51$	$32.4 \pm 31$	$160.8 \pm 43$	$64.7 \pm 39$	63.1
Total	$417.6 \pm 81$	$303.2 \pm 48$	$114.6 \pm 30$	$221.3 \pm 19$	$196.3 \pm 33$	46.0

<sup>a</sup> The annual global mean is given along with the ( $\pm$ ) standard deviation (i.e. associated with ozone variability).

<sup>b</sup> Long-term ozone forcing due to methane chemistry-climate feedback.

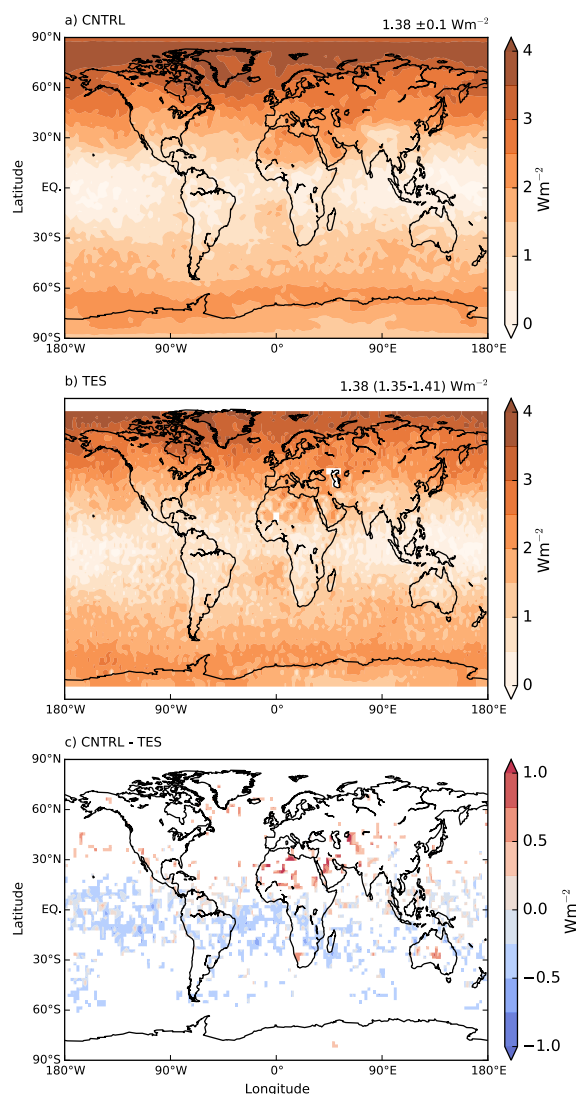


Figure 1. Comparison of the annual mean ozone radiative effect between (a) the CNTRL simulation and (b) the Tropospheric Emission Spectrometer (TES) from July 2005 until June 2008 (05–08). (c) CNTRL simulation bias compared to the TES. Differences are masked for the  $\pm 1.96$  standard error within the three years observed range.

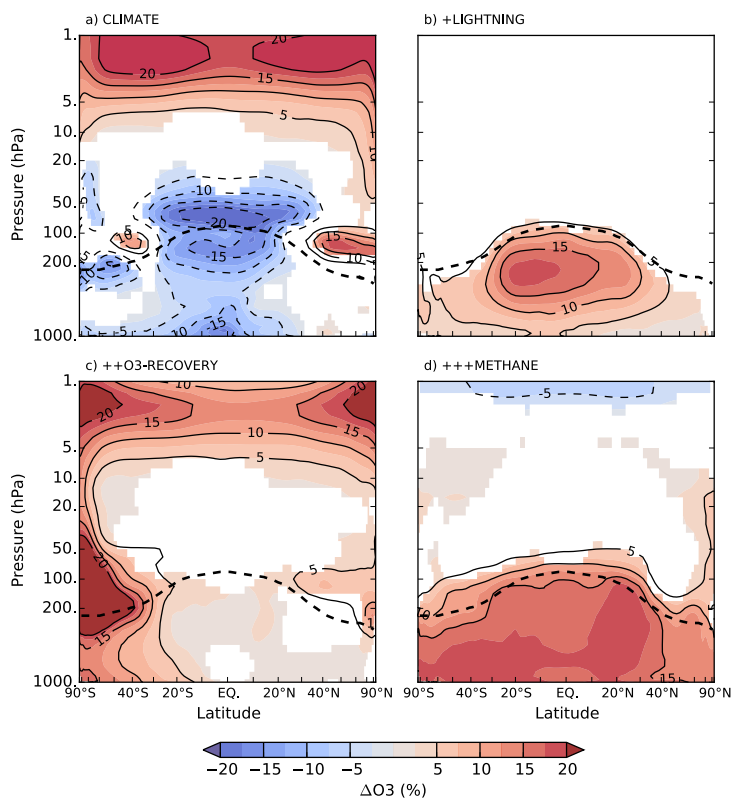


Figure 2. Changes in annual and zonal mean ozone due to (a) CLIMATE (b) +LIGHTNING, (c) ++O<sub>3</sub>-RECOVERY, and (d) +++METHANE by successively adding each individual perturbation to the CNTRL simulation. Contour colours are for statistically significant changes at the 95 % confidence interval using two-tailed Student's t test. The black solid line represents the chemical tropopause based on the CNTRL 150 pbb ozone contour.

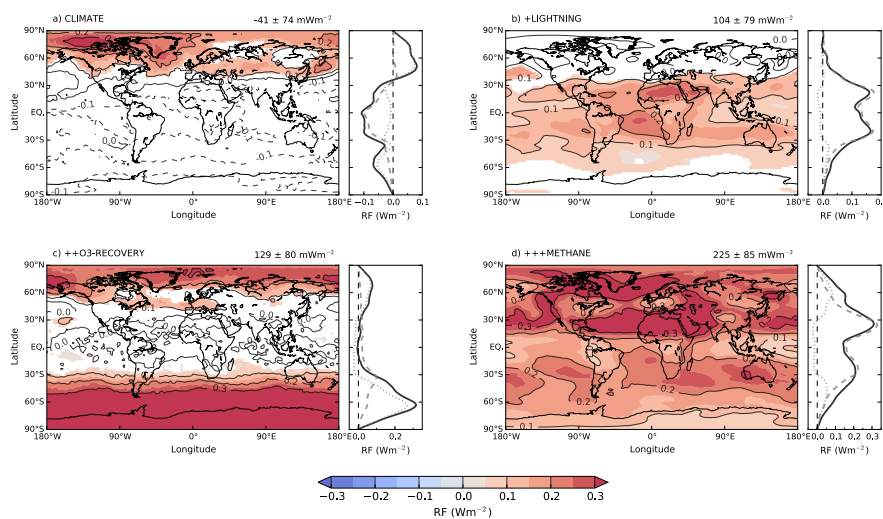


Figure 3. Annual mean maps of ozone radiative forcing (whole atmosphere) due to (a) CLIMATE (b) +LIGHTNING, (c) ++O<sub>3</sub>-RECOVERY, and (d) +++METHANE. Contour colours are for statistically significant changes at the 95 % confidence interval using two-tailed Student's t test. The annual and global mean is shown on the top right corner ( $\text{mWm}^{-2}$ ). Right panels show zonal mean ozone forcings for the whole atmosphere (solid black), troposphere (dashed grey), and stratosphere (dotted grey). The zonal mean forcings are latitudinally-weighted, i.e.  $\cos(\text{latitudes})$ .

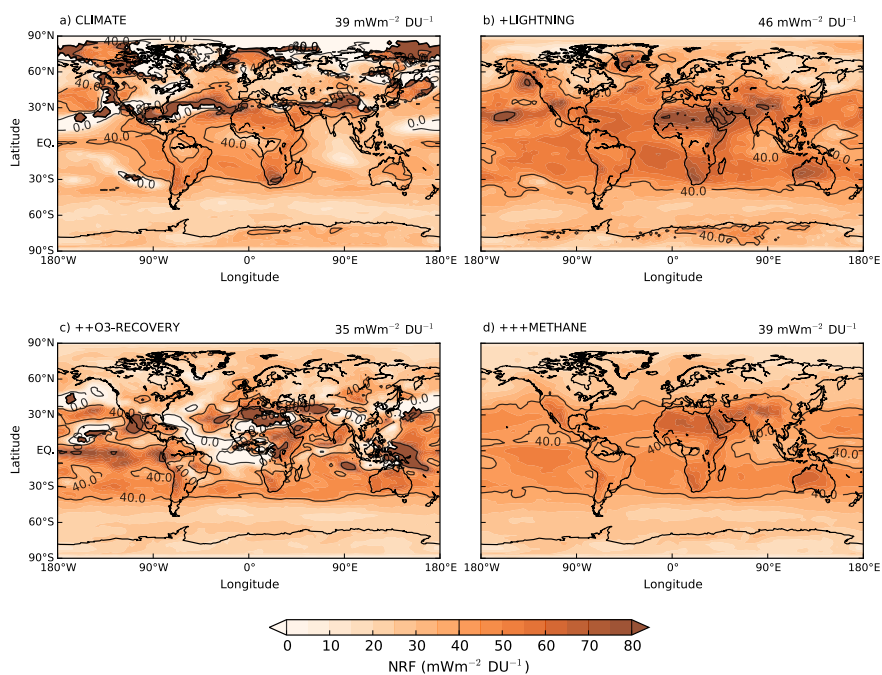


Figure 4. Annual mean maps of normalised tropospheric ozone radiative forcing (i.e. divided by the tropospheric column ozone change) due to (a) CLIMATE (b) +LIGHTNING, (c) ++O3-RECOVERY, and (d) +++METHANE. The annual and global mean is shown on the top right corner ( $\text{mWm}^{-2}$ ).

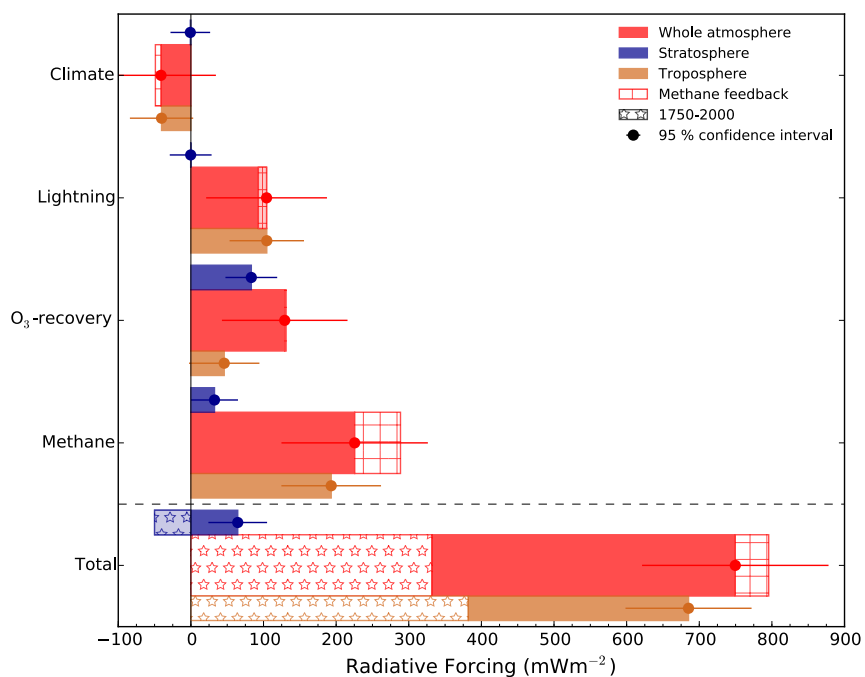


Figure 5. Ozone radiative forcings by drivers (2000–2100;  $\text{mWm}^{-2}$ ). Tropospheric (brown), stratospheric (blue) and net (whole atmosphere, red) forcings are shown. Associated ozone forcings to methane feedback (square-hatched) are shown along with the net forcings. The overall ozone forcing (TOTAL) is also scaled to 1750 (1750–2000; star-hatched). Dots and error bars indicate the mean and the 95 % confidence intervals of the forcings respectively (sources of uncertainty are detailed in Sect. 5).